Aus der Klinik für Allgemein-, Viszeral- und Kinderchirurgie
(Prof. Dr. M. Ghadimi)
der Medizinischen Fakultät der Universität Göttingen

Tumor vessel normalization through inhibition of glycolysis in colorectal carcinoma

INAUGURAL-DISSERTATION

zur Erlangung des Doktorgrades
der Medizinischen Fakultät der
Georg-August-Universität zu Göttingen

vorgelegt von

Shuang Fan

aus

Harbin, China

Göttingen 2023

Dekan: Prof. Dr. med. W. Brück

Betreuungsausschuss

Betreuer*in: PD Dr. med. Dr. rer. nat. Lena-Christin Conradi

Ko-Betreuer*in: Prof. Dr. M. Björn Chapuy

Ko-Betreuer*in (optional): Dr. rer. nat. Tiago De Oliveira

Prüfungskommission

Referent*in: PD Dr. med. Dr. rer. nat. Lena-Christin Conradi.

Ko-Referent*in: Prof. Dr. med. Björn Chapuy

Ko-Referent*in (optional):

Drittreferent*in: …..……..

Datum der mündlichen Prüfung: …..……..

Hiermit erkläre ich, die Dissertation mit dem Titel "Tumor vessel normalization effects in colorectal carcinogenesis and its therapy through inhibition of glycolysis " eigenständig angefertigt und keine anderen als die von mir angegebenen Quellen und Hilfsmittel verwendet zu haben.

Göttingen, den …… ……

(Unterschrift)

Die Daten, auf denen dieser Artikel beruht, sind nicht veröffentlicht worden:

Edelmann M, Fan S, De Oliveira T, et al.

Table of Contents

List of Figures

List of Tables

List of Abbreviations

ACAD9	Acyl-coA dehydrogenase family member 9
APC	Adenomatous polyposis coli
ATM	Ataxia telangiectasia mutated
BSA	Bovine serum albumin
CC	Colon cancer
CD31	Cluster of Differentiation 31
CRC	Colorectal cancer
CRCLM	Colorectal cancer liver metastasis
CRT	Chemoradiotherapy
CT	Chemotherapy
CTB	CellTiter blue assay
DSBs	DNA double-strand breaks
DMSO	Dimethyl sulfoxide
DMEM	Dulbecco's modified eagle medium
EDTA	Ethylenediaminetetraacetic acid
ECs	Endothelial cells
ECGM2	Endothelial cell growth medium 2
ECGS	Endothelial cell growth supplement
ES	Enrichment score
FBS	Fetal bovine serum
GSEA	Gene set enrichment analysis
HR	Homologous recombination
HSC70	Heat shock protein 70
IF	Immunofluorescence
IR	Ionizing radiation
IHC	Immunohistochemistry
KRAS	Kirsten rat sarcoma viral oncogene homolog
LDHA	Lactate dehydrogenase A
LM	Liver metastasis
mCRC	Metastatic colorectal cancer
NDUFB6	NADH: ubiquinone oxidoreductase subunit B6

NF-κB	Nuclear factor kappa B
PBS	Phosphate-buffered saline
PDOs	Patient-derived organoids
PDX	Patient-derived xenograft
PFA	Paraformaldehyde
PFKFB3	6-pPhosphofructo-2-kKinase/fFructose-2,6-bBiphosphatase 3
PS	Penicillin-streptomycin
RC	Rectal cancer
RIPA	Radioimmunoprecipitation assay
RT	Radiation therapy
RTCA	Real-time cell analysis
ROS	Reactive oxygen species
SDS	Sodium dodecyl sulphate
SEM	Standard Error of the Mean
TBST	Tris-buffered saline with tween 20
TECs	Tumor endothelial cells
TP53	Tumor protein 53
TVN	Tumor vessel normalization
TME	Tumor microenvironment
TNM	Tumor, node, metastasis
TUNEL	Terminal deoxynucleotidyl transferase dUTP Nick End Labeling
UICC	Union for international cancer control
VEGF	Vascular endothelial growth factor
VCO	Vessel co-option
WNT	Wingless-integrase-1
3PO	2E-3-(3-Pyridinyl)-1-(4-pyridinyl)-2-propen-1-one
5-FU	5-Fluorouracil
γ-H2AX	Phosphorylated H2AX on S319

1 Introduction

1.1 Definition and epidemiology of colorectal cancer (CRC)

Globally, CRC occupies the second position in terms of cancer-related fatalities, while simultaneously securing third in prevalence among malignancies (Bray et al. 2018). Over the last 25 years, the occurrence of CRC in the older populations (≥ 65 years) has seen a decline, however, its incidence has increased among young adults in Europe (Vuik et al. 2019). Unfortunately, the precise reasons behind this increase are still unclear, however, there are predictable underlying contributors like genetics, age, obesity, lack of exercise, smoking, and poor dietary choices that compromise the immune system and intestinal flora, leading to genetic and epigenetic modifications in colorectal epithelial cells (Akimoto et al. 2021).

The Union for international cancer control (UICC) classification scheme (ranging from I to IV) at time of diagnosis aims to classify the patients according to the estimated and expected survival, with 5-year relative survival varying from 91 % for cases that are localized to 14 % for instances of distant metastasis (Siegel Rebecca L. et al. 2023). Synchronous liver metastases were detected in 75 % of CRC cases, while synchronous lung metastases were observed in 24 % (Robinson et al. 2017) (Figure 1). The development of CRC is generally at a slow pace, usually taking several years and commonly starting as a polyp in the lining of the rectum or colon (Grinnell and Lane 1958; Muto et al. 1975).

The main molecular pathway leading to colorectal carcinogenesis has been well described (Keum and Giovannucci 2019). The tumor suppressor gene adenomatous polyposis coli (APC) is essential for restraining cancer cell proliferation and safeguarding against cancer initiation when it becomes inactivated. This gene mutation occurs in 80 % of intestinal tumors and significantly influences cell proliferation and cancer progression (Fearon 2011). After the inactivation of APC, mutations in tumor protein 53 (TP53) and Kirsten rat sarcoma viral oncogene homolog (KRAS) are commonly noted as persistent occurrences in the progression intestinal neoplasms (Fujii et al. 2002; Vogelstein et al. 1988). Furthermore, another common pathway for colorectal carcinogenesis is DNA mismatch repair (MMR), a system disorder that results in satellite instability (Boland and Goel 2010; Fishel 1998). Additionally, hypermethylation of the CpG islands (Jabbari and Bernardi 2004), chronic enterocolitis (Sturlan et al. 2001), molecular activation of signal transducer, nuclear factor

kappa B (NF-κB) and activator of transcription 3 (Grivennikov and Karin 2010; Rezapour et al. 2016; Yu et al. 2007), all these factors might contribute to CRC.

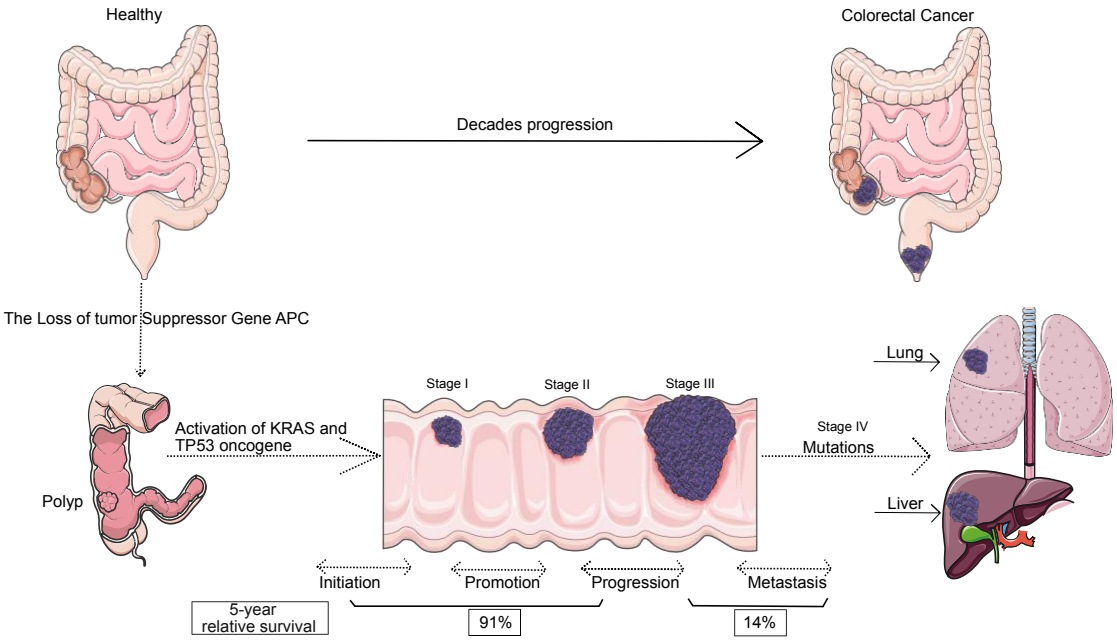

Figure 1: Stages and progression of CRC. Most CRC develop from polyp lesions formed in the epithelial line of the intestinal mucosa. In the context of CRC, mutations in key the activate oncogenes KRAS and tumor-inhibiting genes TP53 are frequently detected. The figure was created using smart.servier.com (accessed on 1 July 2023).

1.2 Standard treatment of CRC and its limitations

The CRC staging can be categorized utilizing the tumor, node, metastasis (TNM), which evaluates tumor dimensions (T), lymph node engagement (N) as well as the detection of remote metastasis (M). The stages are as follows: Stage 0 refers to cancer in its earliest form, known as 'in situ' (Tis, N0 and M0). Stage I represents cancer that is localized (T1, T2, N0 and M0). The stage II corresponds to early advanced local cancer (T2, T3, T4, N0 and M0). The stage III signifies late stage of advanced local cancer (T1-T4, N1-N3 and M0). Finally, stage IV indicates cancer that has metastasized (T1-T4, N1-N3 and M1). Additionally, UICC classification system, which includes TNM staging along with other important predictive elements such as tumor grade, histological subtype, and specific molecular markers. Currently, worldwide, patients exhibiting a restricted count of metastases and the technical possibility for surgical resection may become completely cured, whereas for patients with widespread metastasis and without the technical possibility for surgical resection palliative therapy might be a more appropriate strategy (Dekker et al. 2019; Pox et al. 2013). Treatment decisions for CRC are influenced by various factors such as the specific subtype or histological

classification of CRC and stage of cancer, the patients physical condition, and possible therapy-related side effects (Dekker et al. 2019).

To date, treatment is mainly relying on surgical excision and/or chemotherapy (CT) and/or radiotherapy (RT). Due to anatomical and biological differences, colon cancer (CC) is primarily treated with surgical intervention and depending on the TNM-stage optional adjuvant chemotherapy, while rectal cancer (RC) is commonly treated through either surgery combined with RT or chemoradiotherapy (CRT) (Dekker et al. 2019). Studies have shown that laparoscopic surgery, when performed by trained surgeons, is as safe as conventional surgery regarding the operative part of the treatment strategy and offers long-term oncological safety for CRC, along with notable short-term benefits like reduced blood loss and shorter incision lengths (Green et al. 2013; Kearney and Coffey 2015; Martínez-Pérez et al. 2017). Among all available treatment modalities, the surgical resections seems to be the only definitive curative treatment, however, because many patients suffer from advanced CRC upon diagnosis, the vast bulk of patients require additional approaches, such as adjuvant therapy (Siegel R. L. et al. 2020). Nonetheless, all treatment methods come with adverse effects and complications. Apart from the direct general surgical complication, such as hemorrhage, infection and pain, surgical resection for CRC can also lead to surgery specific complications such as blood clots, anastomosis leakage, intestinal dysfunction and malnutrition, which can not only be life-threatening but also severely affecting patient's overall state of health (Bryant et al. 2012; Dekker et al. 2019; Lange and van de Velde 2011).

As previously described, the treatment strategies for rectal and CC differ according to tumor localization and patients' anatomical characteristics (Heald and Moran 1998; Iacopetta 2002; Li and Lai 2009). The treatment of RC with preoperative UICC-stages I is based on primary resection and, depending on the pathological TNM, additional therapies. Patients with pT1/2 N0 M0 situations receive the medical aftercare. In case of pT3/4 N0 M0 or nodal positive situations an adjuvant treatment usually consisting of CRT.

The rectum can be partitioned into three distinct segments based on their proximity to the anal verge: upper third (typically extending in the range of 10 to 15 cm beyond anal verge), middle third (ranging approximately between 5 and 10 cm beyond anal verge), lower third (typically spanning in the range of 0 to 5 cm beyond anal verge), and the tumor's location within these thirds significantly influences the choice of treatment approach for RC. In stage II-III, surgery continues to play a crucial role, but it is, depending on the primary tumor localization usually combined with additional neoadjuvant in case of tumor localization in the lower and middle thirds or adjuvant treatment in case of tumor localization in the upper

third to enhance the treatment's efficacy (Sauer R et al. 2004; Tamas et al. 2015; Tiefenbacher and Wenz 2001). Treatment for advanced RC, individual therapy strategies like surgery and CRT. Additionally, targeted therapies and immunotherapy might be considered. It is crucial to recognize that treatment plans are personalized to suit individual factors and circumstances (Hernandez Dominguez et al. 2023; Ronnekleiv-Kelly and Kennedy 2011). Neoadjuvant therapy includes RT and CRT. Pre-operative and post-operative RT or CRT can effectively reduce tumor recurrence. A review article published in 2018 indicates that patients diagnosed with locally advanced CRC can safely prolong the interval beyond 8 weeks between preoperative neoadjuvant CRT and surgery. This extended waiting period has shown to effectively shorten the intraoperative procedure time and lower the risk of postoperative complications (Du et al. 2018).

As previously described, regarding RC, RT is usually used either pre-operatively (neoadjuvant therapy) to reduce tumor volume and increase respectability or post-operatively (adjuvant therapy) to destroy the possibly remaining tumor cells (Tiefenbacher and Wenz 2001). Yet, the toxicity of RT has been recognized since the early 1900s and should not be neglected. The manifestations of toxicity are diversified and vary in severity. Frequent and bothersome consequences of lower abdominal and perianal radiation often include diarrhea (Sauer R et al. 2004). Also, surgical resection comes along with adverse side effects. Low anterior resection syndrome manifests in approximately 40 % of patients and the main symptoms are fecal incontinence and abdominal pain (Croese et al. 2018). Some patients may also develop genitourinary disorders and/or sexual dysfunction (Costa et al. 2018; Hendren et al. 2005).

Simultaneous CT and RT are commonly employed to augment treatment effectiveness (Graham and Cassidy 2012; Sauer RT et al. 2004). In recent decades, adjuvant CT has emerged as the customary approach for stage III CC or RC in the upper third. The choice of CT drugs may vary slightly for CRC. Drugs like 5-fluorouracil (5-FU), capecitabine, platinum-based drugs and oxaliplatin are commonly used for CC, inhibiting cancer cell growth by interfering with DNA synthesis. 5-FU and capecitabine are also used for RC, often combined with RT to improve treatment effectiveness (Koopman et al. 2007; Seymour et al. 2007; Xie et al. 2020). Although these chemotherapeutic drugs can extend the OS of patients to nearly 20 months, their limitations and side effects cannot be ignored, such as unpredictable innate acquired resistance and systemic chronic toxicity (Xie et al. 2020). For example, oxaliplatin is one of the most used chemotherapeutic drugs, but its side effects on sensory neuropathy are a severe problem (Dekker et al. 2019; Meyers et al. 2017). Often, combination treatments, where several drugs are administrated (*e.g.* FOLFOX – a

combination of 5FU, oxaliplatin, and folic acid) will cause stronger side effects, such as severe leucopenia, mucosal ulcerations, increased risk of systemic infection and digestive problems, to cite some (Salehifar et al. 2019). Therefore, new treatments should be developed to improve the current treatment options.

Lately, immunotherapy has shown promising results, achieving sustained and persistent improvement in a subset of patients, compared to other treatments on metastatic colorectal cancer (mCRC). However, not all patients have benefit on this treatment, which has limited the widespread use of this specific immunotherapy (Ganesh et al. 2019).

Liver metastasis (LM) is a frequent metastasis site of CRC (Fleischer et al. 2023; Robinson et al. 2017). Surgical resection was established as a successful therapeutic approach for colorectal cancer liver metastases (CRCLM) during the 1980s. However, only 15-20 % of LM can be resected when detected at initial diagnosis, and a significant percentage will have a relapse after surgery (Hu et al. 2021). Recently studies have pointed out that individuals diagnosed with CRC and isolated liver metastases, after appropriate chemotherapy, can be surgically resected and achieve a 50 % survival rate within a 5-year span (Brouquet et al. 2011; Graham and Cassidy 2012).

Currently, a major challenge in treating CRCLM is the emergence of drug resistance, resulting in treatment failure. This resistance stems from a multitude of factors, such as the diverse nature of CRCLM, genetic mutations, tumor microenvironment (TME), and the changes in cancer cell behavior. Consequently, achieving long-term suppression of all tumor cells becomes arduous, allowing some cancer cells to evade treatment and leading to tumor recurrence or ongoing progression (Leenders et al. 2004; Rubenstein et al. 2000). The fundamental mechanisms underlying acquired resistance include the neoplastic cells' ability to modify cellular apoptotic pathways as well as the phenomenon of vessel co-option (VCO) (Bridgeman et al. 2017; Keunen et al. 2011; Leenders et al. 2004; Rubenstein et al. 2000; Wang Q et al. 2022). VCO means in which malignant cells, instead of relying on angiogenic process, seize control of the pre-existing vascular network in host organs to establish their own blood supply. This phenomenon is more common in tissues and organs with rich vascular supply, like the hepatic parenchyma (Donnem et al. 2013; Latacz et al. 2020).

VCO is a phenomenon that usually can be identified through basic histological analysis and plain light microscopy. One of its distinctive characteristics is that cancer cells utilize the vasculature of the host organ instead of destroying them (Kuczynski et al. 2019; van Dam et al. 2017). Recent scientific inquiries, a correlation has been established between VCO and pericytic mimicry migration (Barnhill et al. 2018; Bentolila et al. 2016), this might increase

the tumor's aggressiveness (Lugassy et al. 2020). Additionally, evaluation of CRCLM at a single cell level showed that specific metabolic changes and activation of the wingless-integrase-1 (WNT) signaling pathway were identified, which are linked to the phenomenon of VCO (Fleischer et al. 2023).

1.3 Tumor angiogenesis and anti-angiogenic therapy

Tumor angiogenesis denotes the formation of novel blood vessels within tumors, typically exhibiting abnormal characteristics. This process promotes the advancement of tumor development and the dissemination of cancerous cells to remote locations (Hashizume et al. 2000; Trédan et al. 2007). During tumor development, abnormal and inefficient vessels grow within the tumor and its microenvironment, reduced oxygen levels, decreasing pH and increasing interstitial pressure in the tumor environment. In this process, tumor endothelial cells (TECs) are further stimulated to migrate and proliferate forming new vessels. This phenomenon commences with the release of proangiogenic substances from cancerous and surrounding stromal cells (*e.g.* macrophages, fibroblasts, etc.) (Chang et al. 2000; Gacche 2015; Nowak-Sliwinska et al. 2018).

Anti-angiogenic therapy as a concept was initially put forth by Folkman and his team. In 1971, suggesting a strategy to impede tumor growth by disrupting existing blood vessels within the tumor tissue and restraining the creation of new vascular, which reduces the thereby reducing oxygen levels and supply of essential substances supply to the cancer cells (Folkman J. 1989; Hanahan D. and Folkman 1996). Since then, there has been a shift in tumor treatment approaches for certain patients. Instead of solely relying on traditional CRT, which primarily targets cancer cells, there has been an increasing emphasis on anti-angiogenic therapy. This approach is a new field of tumor treatment and involves targeting the blood vessels that delivers oxygen and nourishment to tumors. This treatment strategy is applicable to specific subsets of patients and may not be universally applicable to all cases (Baluk et al. 2005; Boehm-Viswanathan 2000; Folkman Judah 2007; Grothey and Galanis 2009).

To induce angiogenesis, tumors secrete elevated amounts of growth factors with pro-angiogenic elements, containing vascular endothelial growth factor (VEGF) and angiopoietin 1, along with other related factors (Carmeliet and Jain 2011; Gupta and Qin 2003). The excessive and aberrant tumor angiogenesis is primarily provoked by a disruption in pro-angiogenic factors resulting from the overproduction of VEGF triggered by hypoxia (Carmeliet 2005; Yancopoulos et al. 2000). Tumor angiogenesis encompasses a multifaceted series of sequential events, which can be categorized into four basic steps: (1) basement

membrane degradation, (2) endothelial cells (ECs) migration, (3) proliferation of ECs at the leading edge of migration (4) new vessel lumen formation, which finally results in new vessel formation (Bussolino et al. 1997). Although various molecular mediators play crucial roles in regulating cancer angiogenesis, VEGF has emerged as the most extensively investigated factor (Gupta and Qin 2003). Consequently, after Folkman and his team's recognition of the critical function of VEGF in driving tumor angiogenesis, they conducted experiments using VEGF inhibitors to treat tumors and illustrated the viability of utilizing VEGF as a therapeutic target to impede tumor growth and angiogenesis (Folkman J. 1989). Several decades after Folkman et al.'s seminal observations, targeted therapeutics, such as bevacizumab, have gained approval for utilization in cancer treatment (Hurwitz et al. 2004). Nevertheless, the treatment results shown are still not satisfactory (Lopes-Coelho et al. 2021). This is primarily due to the limited comprehension of the molecular process underlying tumor vascularization, which hampers the achievement of success in this treatment approach. Furthermore, by targeting the blood supply of angiogenesis, the transportation of chemotherapeutic drugs to the tumor is impeded, which not only reduces the efficacy of chemotherapeutic drugs but also enhances the tumor's resistance (Rohlenova et al. 2018). Based on these facts, a new therapeutic approach has been proposed: instead of inhibiting tumor angiogenesis, it would be favorable to promote the tumor vessel normalization (TVN) to improve blood perfusion, this process aims to alleviate hypoxia and decrease interstitial pressure, reduces the infiltration and dissemination of malignant cells. By improving blood perfusion through TVN, the transport of CT agents to the lesion site is enhanced, allowing for better drug distribution and increased effectiveness (Cantelmo A. R. et al. 2016; Conradi et al. 2017). Additionally, elevated oxygen levels within the TME could also promote irradiation effects via reactive oxygen species (ROS)-mediated DNA damage on the cancer cells (Jing et al. 2019).

1.4 Tumor vessel normalization as a breakthrough for new therapeutic options

With a better understanding of CRC and its microenvironment, it is now well known accepted that the hypoxic condition experienced by tumor cells contributes to tumor progression, metastasis, while also impairing tumor-infiltrating immune cell activity, further enhancing the malignant phenotype. Moreover, highly hypoxic conditions also diminish the effectiveness of both RT and CT treatments (DeClerck and Elble 2010; Hockel et al. 1999; Semenza G. L. 2010). Research has shown that the hypoxic conditions within the TME can lead to the increased expression of transcription factors known as hypoxia-inducible factors, which are crucial for enabling malignant cells to survive in low-oxygen environments by activating genes related to glucose uptake (Rankin and Giaccia 2016; Semenza Gregg L. 2012). Additionally, it has been observed that the hypoxic environment within tumors can promote an immunosuppressive phenotype, including a reduction in the penetration of $CD8^+$ cells, along with a decrease in the regulatory T cell activity (Hatfield et al. 2015). The production of ROS is the primary mechanism through which RT exerts its therapeutic effect, as shown by the current research (Kim W et al. 2019). However, this also explains why hypoxic tumors, with a lack of sufficient oxygen for ROS generation, are resistant to RT.

This might be one reason, why anti-angiogenic therapies, which aim to reduce tumor angiogenesis and thereby limit tumor access to nutrients, have not been as effective as anticipated. Instead, these therapies often result in a more hypoxic TME, which might result in the development of more CT resistant tumor cells and contribute to vascular leakage and intracellular infiltration (Cully 2017). Considering this, by TVN to restore intra-tumor perfusion to potentially reduce metastasis, enhancing drug transport and increasing CT response (Cantelmo A. R. et al. 2016; Park et al. 2016). This method has been showed promising results in comparison to traditional anti-angiogenic therapies (Cantelmo A. R. et al. 2016; Conradi et al. 2017). Moreover, TVN could also promote RT effects via ROS-mediated DNA damage on the cancer cells (Jing et al. 2019). Molecularly, TVN can be achieved by interfering with the metabolic phenotype of ECs, which are highly dependent on glycolysis for their proliferation (Cantelmo A. R. et al. 2016).

1.5 Induction of TVN by inhibition of glycolysis

In non-transformed healthy cells, the tricarboxylic acid cycle serves as the primary pathway for energy generation. However, in 1956 Warburg et al. discovered that some normal non-transformed cells and most tumors can reach their energy demands through glycolysis instead (Warburg 1956). Since then, there has been a growing understanding of tumor metabolism and its key regulators. Among the regulators in focus, a glycolytic activator, 6-phosphofructo-2-kinase/fructose-2,6-biphosphatase 3 (PFKFB3) stands out as a central player. PFKFB3 drives tumor progression by activating phosphofructokinase-1, promoting the synthesis of fructose-2,6-bisphosphate, and consequently enhancing glycolytic activity (Lu L et al. 2017). Increased PFKFB3 expression is observed in several ailments, including CRC (De Oliveira et al. 2021). Therefore, targeting PFKFB3 has arisen as a hopeful therapeutic approach for CRC treatment.

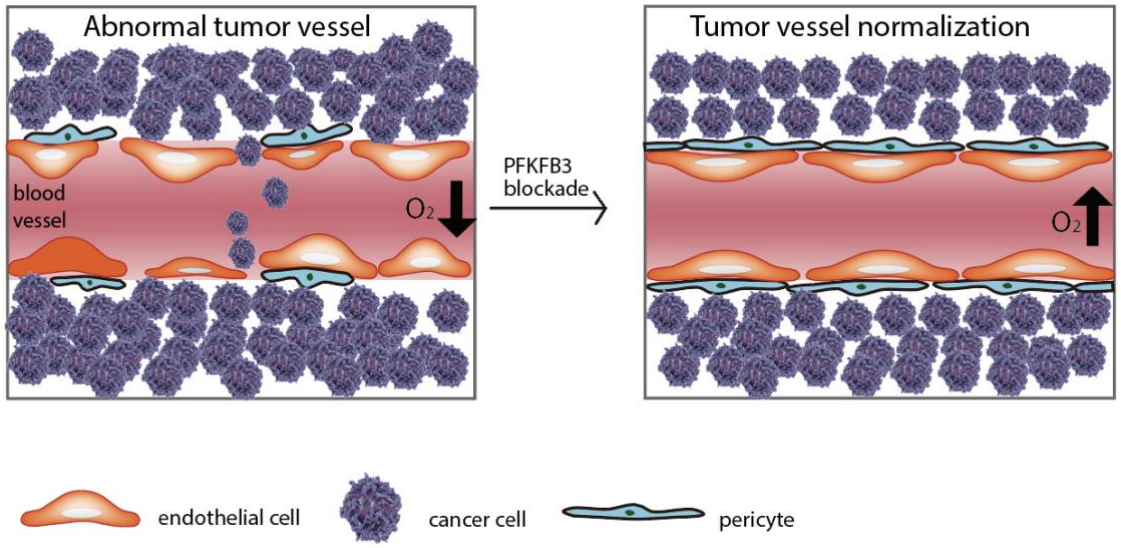

Figure 2: TVN. Reinforcing the vascular barrier and restoring normalcy to tumor vessels by inhibiting PFKFB3 enhances vessel perfusion. This strengthened barrier diminishes cancer cell intravasation, curtails metastasis, elevates oxygen levels, and enhances the response to chemotherapy.

VE-cadherin, a central player in preserving the integrity of cellular connections and maintaining endothelial stability, is predominantly expressed in ECs (Vestweber 2008). Mechanistically, inhibiting PFKFB3 can regulate the endocytosis of VE-cadherin, exerting an influence on the metabolism and function of tumor ECs. These effects contribute to maintaining vascular integrity and tightness, reducing vascular tortuosity and ultimately improving tumor vascular perfusion (Cantelmo A. R. et al. 2016; Conradi et al. 2017) (Figure 2). Furthermore, suppressing PFKFB3 can reduce NF-κB signaling, which is recognized for its role in suppressing pericyte coverage (Caporali et al. 2015). Furthermore, the

normalization of the endothelial cell layer leads to improved oxygenation and increased blood flow. This, in turn, promotes enhanced pericyte coverage, stabilizes the ECs layer and contributes to the establishment of the vascular network in the organ. (Hutter-Schmid and Humpel 2016).

In summary, abnormal tumor vasculature amplifies cancer cells' capacity to metastasize and elude immune surveillance, as well as to resist CRT. For these reasons, TVN is a promising anti-tumor treatment option. It is reasonable to hypothesize that TVN can reduce the hypoxia levels in the TME, enhancing the effect of CRT, inhibiting tumor cell metastasis.

1.6 PFKFB3 inhibition combined with RT in CRC treatment

In the complex scenario of tumor growth and progression, the inhibition of PFKFB3 using a compound known as 2E-3-(3-Pyridinyl)-1-(4-pyridinyl)-2-propen-1-one (3PO) demonstrated a potential therapeutical approach to block tumor growth and improve vascular function by promoting TVN (Cantelmo A. R. et al. 2016; Clem et al. 2008; Conradi et al. 2017). Solid tumors' blood vessel system is a fundamental component in determining their advancement and propensity for metastasis. Abnormal vessel formations usually create a poorly oxygenated and perfused TME that supports tumor invasiveness and resistance to treatment (Bertout et al. 2008). TVN aims to restore functional blood vessels, improve tumor oxygenation and potentially enhance the efficacy of cancer treatments like CRT (Moeller et al. 2007). TVN might support ROS formation and fixation during RT and improve drug distribution in case of CT in tumor tissue by improving tumor perfusion (Jain 2014; Wilson and Hay 2011). Therefore, the utilization of 3PO as an inhibitor of PFKFB3 holds the promise to enhance the efficacy of CRT.

RT is employed to inflict damage on malignant cells, primarily by inducing DNA double-strand breaks (DSBs) (Rupnik et al. 2010). After RT, tumor cells activate ataxia telangiectasia mutated (ATM) kinase, leading to γH2AX formation, which then forms a feedback loop. γH2AX serves as a rapid DSB-recruitment marker for DNA damage. It is of utmost importance in the restoration of DNA damage in irradiated tumor during cancer treatment (Cuadrado et al. 2006; Rupnik et al. 2010). Repair of DSBs after damage relies mainly on the homologous recombination (HR) as well as non-homologous end-joining (Huertas 2010). Recently, Gustafsson and his colleagues suggested that PFKFB3 re-localizes to irradiation-induced nuclear foci in the ATM-γH2AX- mediator of DNA damage checkpoint 1 pathway, facilitating the enlistment of elements associated with HR and helping to reverse cell cycle arrest caused by ionizing radiation (IR) (Gustafsson et al. 2018). Taking advantage of the

possible radio-sensitizing effects of PFKFB3 inhibition, it is conceivable that PFKFB3 inhibitors combined with RT could improve the therapeutic effect (Gustafsson et al. 2018).

The current investigation showcases that the therapeutic efficacy of CRT in CRC treatment can be enhanced by incorporating 3PO into the treatment regimen. Application of 3PO, has promising outcomes with decreased cancer cell invasion and enhanced radiation-induced cellular death. Moreover, neoadjuvant treatment with 3PO *in vivo* induced TVN in RC, ultimately leading to a significant improvement in therapeutic response.

1.7 Aim of this study

CRC is a relevant malignancy with significant mortality and treatment options remain limited (Sung et al. 2021). TVN is a promising strategy that might reduce tumor hypoxia and might improve vessel perfusion, which can result in reduced metastasis and enhanced efficacy of CRT. However, our comprehension of TVN's impact on CRC cells remains incomplete. In this context, the enzyme PFKFB3, which is involved in glycolysis, has surfaced as a potentially advantageous target for cancer therapy. PFKFB3 inhibition has demonstrated the ability to diminish tumor growth in various cancer types (De Oliveira et al. 2021; Matsumoto et al. 2021; Xiao et al. 2021). However, the effects on TVN and CRC cells are yet to be clarified.

In this study, we seek to address several specific questions related to the potential of PFKFB3 inhibition by 3PO in enhancing radiation-induced effects in CRC. The primary aims are as follows: 1. Does PFKFB3 inhibition by 3PO enhance radiation-induced effects *in vitro* using CRC cell lines? 2. Can the effectiveness of 3PO be validated *in vivo* using an established RC patient-derived xenograft (PDX) model? 3. What are the effects of PFKFB3 inhibition on tumor volume and CRC cells? By answering these questions, this research aims to provide valuable insights into pioneering innovative and efficacious therapies for CRC treatment, contributing to the advancement of cancer treatment strategies.

2 Materials and Methods

2.1 Materials

Material and kits are listed in Table 1-8. The standard laboratory equipment and suppliers are provided in the appendix.

2.1.1 Buffers and solutions

Table 1: Buffers and solutions

Blocking solutions	
Western blot	5 % Milk powder in Tris-buffered saline with tween 20 (TBST)
Western blot for phospho-antibodies	5 % Bovine serum albumin (BSA) in TBST
Immunofluorescence (IF)	10 % Fetal calf serum (FCS) in phosphate-buffered saline (PBS)
Cell lysis buffer	
Tris-HCI, PH 7.8	5 ml
NaCl	3 ml
NP-40	1 ml
Aqua dest.	91 ml
Tris, PH 7.8	50 mM
NaCl	250 mM
Ethylenediaminetetraacetic acid (EDTA)	30 mM
Sodium deoxycholate	25 mM
Triton-X 100	1 %
NP-40	0.5 %
Glycool	10 %
Dithiothreitol	1 mM

SDS- Polyacrylamide Gel Electrophoresis 10X running buffer, PH8.3	
Glycin	288.26 g
Tris	60.56 g
Sodium Dodecyl Sulfate (SDS)	20 g
ddH_2O	1.8 L
10X TBST	
Tris, PH 7.5	60.57 g
NaCl	88.66 g
Aqua dest.	Add to 1 L
Tween20	0.1 %
10X Transfer buffer	
Glycin	288 g
Tris	60.4 g
SDS	20 g
ddH_2O	1.8 L
Western blot loading buffer	
20 % SDS	3 ml
Tris, PH 6.8	3.75 ml
Bromphenol blue	9 mg
B-mercaptoethanol	2.4 ml
Glycerol	4.5 ml

2.1.2 Cell culture

Table 2: Cell lines

Cell line	Origin	Culture in	Source
HUVCES	human umbilical vein endothelial cells	1:1 v/v mixture of Endopan 300SL and Medium 199	Dr. Joanna Kalucka (Department of Biomedicne, Aarhus University, Aarhus, Denmark)

RPE-1	human retinal epithelial cell	Dulbecco's modified eagle medium (DMEM): F12 Medium	By Dr. Holger Bastians (Institute for Molecular Oncology, University Medical Center Göttingen, Germany)
HCT-116, HT-29. SW-1463, SW-837.	human CC. human RC.	McCoy's 5A (modified) medium. Leibovitz's L-15 Medium. Both supplement with 10 % Fetal bovine serum (FBS)	American Type Culture Collection (ATCC, Manassas, USA)

All media were additionally enriched within 100 U/ml penicillin-streptomycin (PS) and 2 mM L-glutamine.

Table 3: Media for cell culture

1:1 v/v mixture of Endopan 300SL and Medium 199	
Endopan 300SL	250 ml
Medium 199	250 ml
FBS; Glutamine	20 %; 1 %
Glutamine	1 %
Endothelial cell growth supplement (ECGS)/Heparin	1 ml
DMEM: F12 Medium	
DMEM: F12	500 ml
FBS; Glutamine; PS	10 %; 1 %; 1 %
McCoy's Medium	
McCoy's Medium	500 ml
FBS; Glutamine; PS	10 %; 1 %; 1 %
Leibovitz's L-15 Medium	
Leibovitz's L-15 Medium	500 ml

FBS; Glutamine; PS	10 %; 1 %; 1 %

2.1.3 Chemotherapeutics, inhibitors and chemicals

Table 4: Chemotherapeutics, inhibitors and chemicals

Name	Company
3PO	ChemBridge Corporation (San Diego, USA)
Dimethyl sulfoxide (DMSO)	Sigma-Aldrich (Bornem, Belgium)
0,4 % Trypan Blue	Carl Roth (Karlsruhe, Germany)
Sterile methylcellulose; Radioimmunoprecipitation assay (RIPA); Fibrinogen; Thrombin	Sigma-Aldrich (St. Louis, USA)
FBS	Biochrom (Berlin, Germany)
PS; Medium 199; PBS; DMEM/F12 medium; SuperSignal Pico (SSP)	Gibco, Thermo Fischer Scientific (Waltham, MA, USA)
Endopan 300SL medium	PAN Biotech (Aidenbach, Germany)
ECGS/Heparin	PromoCel (Heidelberg, Germany)
Endothelial cell growth medium 2 (ECGM2)	ECGM2, PromCell (Heidelberg, Germany)

2.1.4 Antibodies

Table 5: Primary antibodies used in western blots

Target	Company	Cat. No.	Organism	Dilution
ACAD9	Proteintech (Germany GmbH, Planegg-Martinsried, Germany)	15770-1-AP	rabbit	1: 800, overnight, 4 °C
β-ACTIN	Cell Signaling (Danvers, USA)	#9587	mouse	1: 2000 overnight, 4 °C

Heat shock protein 70 (HSC70)	Santa Cruz Biotechnoligy, lnc. (Dallas, USA)	Sc-7298	mouse	1: 2000 overnight, 4 °C
Lactate dehydrogenase A (LDHA)	Cell Signaling (Technology, Massachusetts, USA)	P00338	rabbit	1: 1000 overnight, 4 °C
NDUFB6	Proteintech (Germany GmbH, Planegg-Martinsried, Germany)	16037-1-AP	rabbit	1: 2000 overnight, 4 °C

Table 6: Primary antibodies used in histology and immunostainings

Target	**Company**	**Cat. No.**	**Organism**	**Dilution**
Cleaved Caspase 3	Cell Signaling	P42574	rabbit	1: 2000 overnight, 4 °C
γH2AX	Cell Signaling	P16104	rabbit	1: 480 overnight, 4 °C
Terminal deoxynucleotidyl transferase dUTP Nick End Labeling (TUNEL)	Promega	#9FB055	N.A	N.A.

Table 7: Secondary antibodies used in western blots

Target	**Company**	**Cat. No.**	**Dilution**
Goat anti-mouse IgG, IgA, IgM (H+L)	Invitrogen	2087698	1: 2000, 1 h at room temperature
Goat anti-rabbit IgG, (H+L)	Invitrogen	2087715	1: 10,000， 1 h at room temperature

2.1.5 Kits and instruments

Table 8: Kits and instruments

Name	Manufacturer
PerkinElmer Victor X4 (For software table as well)	ibidi Integrated BioDiagnostics, Munich, Germany
LDH Cytotoxicity Detection Kit-PLUS	Roche, Diagnostics, Mannheim, Germany
Neubauer-improved Chamber	Paul Marienfeld GmbH, Lauda-Königshofen, Germany
Leica High Speed EC3 camera; Leica DM IL inverted microscope	Leica Microsystems GmbH, Wetzlar, Germany
Non-adherend squared plastic dishes	Greiner Bio One, Kremünster, Austria
24-well-plates	SARSTEDT, Hildesheim, Germany
96-well black polystyrene microplates	Corning, NY, USA
DeadEnd Fluorimetric TUNEL System kit	Promega, Madison, WI, USA
xCELLigence real-time cell analysis (RTCA) S16 instrument	Both ACEA Bioscience, San Diego, CA, USA
RS 225 X-Ray irradiation system	Medical System, Xstrahl Ltd., Camberly, Surrey, UK
Victor™ multi-label plate reader	PerkinElmer, Inc., Waltham, USA

2.1.6 Software

Table 9: List of software's used

Name	Company
GraphPad Prism™ 9	GraphPad Software, San Diego, CA, USA
Gene set enrichment analysis (GSEA) version 4.1.0	University of California San Diego and Broad Institute, USA
ImageJ 1.53a and 1.43u software	National Institutes of Health, Bethesda, Maryland, USA.
ImageQuant LAS 4000 mini system	GE Healthcare, Wauwatosa, Wisconsin, USA

2.2 Methods

2.2.1 Human cell culture

HUVECs from a single donor's early passages were cultivated in a 1:1 volume ratio blend of Endopan 300SL medium and Medium 199 supplemented with 2 ml of ECGS/Heparin. Human retinal epithelial cell (RPE-1) be cultured in DMEM/F12 medium, to which 10 % FBS and 1 % PS were added. HT-29 and HCT-116 CC cells were maintained in McCoy's medium, 1 % PS and 10 % FBS were added for cell culture. HUVECs, PRE-1, HT-29 and HCT-116 were maintained under conditions of 37 °C and 5 % CO2 in a humidified incubator. SW-1463 and SW-837 RC cell lines were cultivated under conditions of 37 °C and atmospheric. Nourished medium with Leibovitz's L-15 enriched using 1 % PS in addition to 10 % FBS. The *in vitro* exposure to DMSO below a maximum concentration of 0.25 % for the cells.

2.2.2 xCELLigence assay

HCT-116, HT-29, SW-837, SW-1463, RPE-1 cells (1×10^4/100 μL) and HUVECS (1.5×10^4/100 μM) were inoculated into 16-well plates featuring gold-coated microelectrodes at the base, and then maintained under conditions of 5 % CO2 and 37 °C to foster their growth, utilizing the xCELLigence. The system continuously measured cell impedance and recorded every 5 min in 96 h to capture the response to 3PO. After the first readout, inhibitors were introduced into the culture medium and were replenished after a 48 h incubation period. Subsequently, the collected data underwent analysis to generate a cell index employing RTCA software Lite version 1.2. In brief, cell indices were computed by analyzing impedance changes, which are impacted by variations in cell morphology, adhesion, proliferation and structure. Each experimental condition underwent triplicate testing, and the experiments were conducted thrice. Group comparisons were conducted by applying a logarithmic transformation to the data and subsequently assessing the 80 h time node, followed by a t-test analysis.

2.2.3 Cell count assay

12-well plates were used to culture HUVEC, SW-1463, HT-29, and HCT-116 cells, each well containing 1 x 10^5 cells. Following an overnight incubation, cells were administered either DMSO (vehicle) or different concentrations of 3PO at 75, 50, 25 and 10 μM for a 24 h culture period. All cells were maintained for the specified duration without reseeding,

following the exchange of the culture medium, all while 3PO was absent. At predefined time intervals, cell detachment was executed through trypsin treatment, followed by manual cell enumeration utilizing a Neubauer hemocytometer.

2.2.4 CellTiter Blue assay

Following the instructions provided by Promega, located in Madison, USA. In 96-well black polystyrene microplates, cell seeding densities were adjusted to 1 x 10^4 for HT-29, HCT-116, SW-1463 and SW-837 cell lines, while HUVEC cells were inoculated at 1.5 x 10^4 per well. After a 24 h incubation under conditions of 37 °C and 5 % CO2, I administered 100 µl of medium containing 3PO. Cell viability was assessed after 48 h. 1 h prior to the experiment's conclusion, 10 µl of resazurin was integrated into each well, followed by an additional hour of incubation for the cells. Optical density was assessed using a Victor™ multi-label plate reader at 590 nm emission wavelength and 560 nm excitation. When the CellTiter Blue assay (CTB) was performed in combination with irradiation, a RS 225 X-ray irradiation system was used. The cells received 3PO treatment, followed by a 4 h incubation period, subsequently exposed to radiation treatment of 6 Gy. Following the radiation treatment, a 48 h incubation period was observed before conducting the CTB test analysis on the cells. Each condition underwent triplicate testing, with assays conducted on three separate occasions. In comparison to the control group, cell viability is indicated as a percentage (Figure 3).

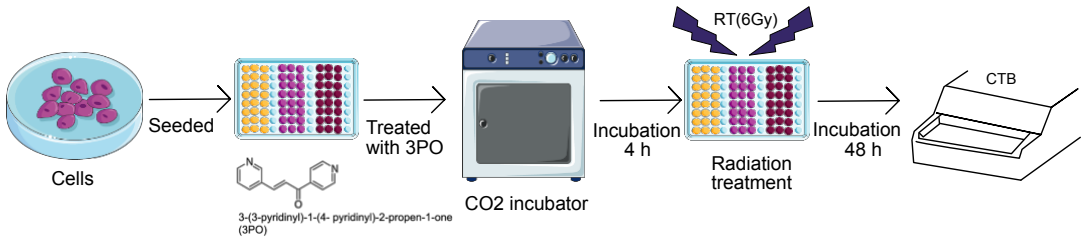

Figure 3. Diagram displaying the *in vitro* radiation assay. Seeded cells were incubated with 3PO for 4h and after irradiated with 6 Gy. Cell viability was measured 48h after. The figure was created using smart.servier.com (accessed on 1 July 2023).

2.2.5 LDH assay

Using the LDH Cytotoxicity Detection Kit-PLUS, the assessment of cell death induced by 3PO followed the manufacturer's guidelines. Briefly, 1.5 × 10^4 HUVECS and 1 × 10^4 (HT-29, HCT-116, SW-1463 and SW-837) cell lines were inoculated into 96-well plates. After a 24 h incubation, added 100 µL medium, within distinct concentrations 3PO. Cytotoxicity was assessed after 48 h. To establish the positive high control, the lysis solution was added

to the designated wells 15 min before the experiment's conclusion, with a volume of 5 μL. Afterward, each well received an aliquot of 100 μL from the reaction mixture and a room temperature incubation followed, shielded from light, in a period of 30 min. Afterward, the VictorTM reader spectrophotometer to quantify the absorbance of the formazan salt at a 490 nm wavelength, following the addition of a 50 μL cessation solution to all wells. LDH assay was performed in conjunction with irradiation, using an RS 225 X-ray irradiation system. Cells were subjected to a 6 Gy single dose irradiation 4 h following the administration of 3PO treatment. Each condition underwent triplicate testing, with three assays conducted.

2.2.6 Invasion assay

The experiment was carried out following detailed (Chen 2005). Firstly, in 1000 μL of the medium, seeded 1×10^5 (HT-29, HCT-116, SW-1463 and SW-837) cells in the Boyden chamber's upper well. Various concentrations of 3PO were introduced to both sides of the chamber and for the invasion assay combined with irradiation. CRC cells were exposed to a sole radiation dose of 6 Gy in 75 ml cell culture flasks. The irradiated cells were then seeded into Boyden chambers. After incubating for 96 h, aspirated the upper chamber medium, collected the lower chamber samples for each condition, comprising cells that were both floating and adherent. Subsequently, centrifuge cells 5 min at 500 G, and then staining them with 0.4 % trypan blue. Cell counting was conducted under a Neubauer-modified chamber and a microscope in a manual manner.

2.2.7 Migration assay

In line with the manufacturer's prescribed protocol (ibid Integrated BioDiagnostics, Munich, Germany), seeded HT-29 and SW-837 cells in μ-Dish™ 35 mm low culture dishes with a cell density of 3×10^4 cells. Upon reaching more than 90 % confluence, we withdrew the silicon scaffold and recorded the migratory behavior of HT-29 cells at 6, 18, 24, 30, 42, 48, and 54 h. SW-837 cells were observed at time points of 6, 18, 24, 30, 42 and 48 h. Images were taken using the Leica DM IL inverted microscope in conjunction with a Leica High-Speed EC3 Camera. Using the RS 225 X-ray irradiation system, cells were irradiated after 4 h of exposure to 3PO, 6 Gy single dose. GraphPad Prism™ and ImageJ 1.53a Software were used for analysis. The test was performed three times. Mobility was determined using the following formula: Mobility (%) = A0 / Ax. The change in the gap area (Ax) corresponds to the gap area (A0) at time 0 h. The resulting percentages describe the migratory capacity of the cells.

2.2.8 Spheroid formation assay

To form spheroids, 5×10^5 HUVECs cells were mixed with ECGM2 10 ml enriched with 2.5 ml (2 % v/w) of sterile methylcellulose. The 25 µl of cell suspension was transferred in multiple passages into non-sticky square plastic trays and inverted (hanging drops) for overnight incubation (16 h). The next day, the formed spheroids were observed under a light microscope (Leica), then gently washed, carefully move the samples to a 50 ml conical tube by adding approximately 10 ml of PBS that contains 10 % FBS. Following centrifugation at 300 G for a duration of 5 min, ECGM2 medium supplemented with 5 mg/ml fibrinogen was gently overlaid on the pellet and mixed without brakes. Next, for coagulation, 0.6 units (6 µl/ml) of thrombin was added and gently mixed again. Then, 500 µL of the mixture containing spheroids was added to a 24-well plate, underwent incubation in that included either DMSO (control) or 3PO. After 24 h, images of the cultures were captured by Leica high-speed EC3 camera and Leica DM IL inverted microscope. To address the treatment of well-established spheroid sprouts, a 24 h sprouting period was permitted, with various concentrations of 3PO for another 24 h. Vascularity was evaluated by quantifying the cumulative shoot length and the number of shoots by ImageJ 1.53a (Schneider et al. 2012). The generation was quantified numerically. At least five spheroids were analyzed for each independent experiment condition.

2.2.9 Colony formation assay

CRC cells were distributed at different densities depending on the cell type (Without RT group: 750 SW-1463, 750 SW-837, 200 HT-29, 500 HCT-116; with RT group: 2250 SW-1463, 2250 SW-837, 600 HT-29, 1500 HCT-116). Cells were inoculated in 6-well plates. Following a 24 h incubate, substituted by medium containing 1, 2.5 and 5 µM 3PO for the combined treatment. Irradiation was performed for 4 h after cells were exposed to 3PO with or without a single dose of 6 Gy irradiation. Maintaining a constant temperature of 37 °C, the plates underwent incubation for 6 days for HCT-116 cells, 7 days for HT-29 cells and 14 days for both SW-1463 and SW-837 cells. Next, all cell lines were fixed using 70 % ethanol, then be stained by crystal violet. The colonies formed were determined under a stereomicroscope. Survivors were defined as colonies comprising more than 50 cells. Data analysis was performed utilizing GraphPad software, located in La Jolla, California, USA. The assays were conducted in triplicates and replicated independently three times.

2.2.10 Patient-derived organoids

The study utilized newly acquired tissue samples from the University Medical Center Göttingen located in Germany (ethical approval UMG Antragsnr. 25/3/17, from 2017), after surgical tumor resection. The establishment and cultivation of intestinal patient-derived organoids (PDOs) followed the previously outlined methodology (De Oliveira et al. 2021). For RNA sequencing analysis three right-sided colon tumors were used. PT16 (ascendens, right-colic flexure), PT12 (coecum) and PT6 (colon ascendens) were all in second passage. The organoids were grown in a medium that contained 30 μM 3PO, and their responses were assessed via light microscopy after a 24 h incubation period. ImageJ 1.43u software was employed for size quantification (Schneider et al. 2012).

2.2.11 Gene set enrichment analysis

GSEA system used in this study was developed by the Broad Institute in the USA and the University of California San Diego (Mootha et al. 2003; Subramanian et al. 2005). Evaluating gene expression data in terms of gene sets to show significant differences between the phenotypes, tumor control and tumor treated with 30 μM 3PO. Utilizing the signal-to-noise ratio as the ranking measure, genes were listed and ranked based on their expression differences between the respective classes. The enrichment score (ES) in GSEA serves as a quantification of how enriched a particular gene set is, whether it's enriched at the upper or lower end of the sorted list. The ES is normalized concerning differences in gene set size creating the normalized ES. A 5% false discovery rate threshold was employed, and the permutation method was designated as "gene set" because less than seven samples were analyzed per condition.

The permutation count was established at 1000. The collection "Biological Process" (c5.go. bp.v7.4.symbols.gmt.txt) contributed by gene ontology (Liberzon et al. 2011; Liberzon et al. 2015).

2.2.12 Western blot

Using a modified RIPA buffer, I gently lysed the samples on ice. The cell lysis buffer sees Table 1 for details. The next steps were performed at room temperature. This lysing process was supplemented within protease and phosphatase inhibitors from Roche diagnostics and achieved by mechanical disruption using a microfine Becton, dickinson and company syringe. The lysate underwent a 10 min centrifugation, then collected the resulting supernatant for immunoblotting. Protein concentrations were assessed following the instructions provided by the manufacturer. Each sample was transferred to a 0.45 μm PVDF membrane after being

loaded with 30 μg of protein onto an 8 % gel-PAGE. The samples were subsequently incubated in TBST containing 3 % non-fat milk (Sigma-Aldrich) for 30. After an overnight incubation, we applied the following primary antibodies: NDUFB6 (1:1000), ACTIN (1:5000), ACAD9 (1:500), LDHA (1:1000) and HSC70 (1:1000). Next, the membranes underwent a 30 min incubation using a secondary antibody linked to horseradish peroxidase. Subsequently, blots were subjected to SSP, then captured by an ImageQuant LAS 4000 mini system. Band intensities were measured utilizing ImageJ 1.5a software.

2.2.13 Histology and immunostainings

After an overnight fixation at 4°C in 4% paraformaldehyde, the PDX tumors were subjected to dehydration, paraffin embedding, and subsequent slicing into 2 μm sections. Allowing for an overnight drying period at 37°C, followed by sequential washing with xylene and varying ethanol concentrations. The sections were boiled in Tris-EDTA (pH 8.5) for 45 min to break the cross-link formed by formalin fixation. The previously published protocols for histological procedures and immunostaining techniques have been followed in this study (Cantelmo A. R. et al. 2016). Immunostainings were done with the following antibodies: CD-31 (BD Biosciences, 1:500), Ki-67 (Thermo Fisher Scientific, 1:200), aSMA, cleaved caspase 3, γ-H2AX (all, 1:500, from Cell Signaling Technology). Mount with DAPI (Invitrogen) was used for IF samples. Tumor necrosis was evaluated on paraffin sections stained with hematoxylin and eosin, quantifying the necrotic portion as a percentage of the overall tumor area.

2.2.14 TUNEL assay

TUNEL analysis was conducted with paraffin sections, following the protocol outlined in the manufacturer's manual for the DeadEnd Fluorimetric TUNEL System Kit.

2.2.15 Statistical analysis

The data were presented as Mean ± SEM (Standard Error of the Mean). Statistical analyses, as specified in the figure captions, were conducted using GraphPad Prism™ 9, employing either a t-test or a two-way ANOVA, depending on the sample size. Specifically, a t-test was applied when the sample size was 2 (n=2), while a two-way ANOVA was used for sample sizes greater than 2 (n>2). Denoted as: ****$p < 0.0001$, ***$p < 0.001$, **$p < 0.01$, *$p < 0.05$, unless otherwise stated.

3 Results

3.1 Glycolysis inhibitor 3PO reduces CRC cell viability in a concentration-dependent manner

3PO has been well recognized and used as an inhibitor of glycolysis (Cantelmo A. R. et al. 2016; Clem et al. 2008; Schoors et al. 2014). While there are no clear findings on what impact inhibition of PFKFB3 has on the treatment of CRC. Therefore, I employed xCelligence assay, cell counting, CTB and LDH assays to comprehensively evaluate the viability and cell death rates of CRC cells (CC cells HT-29, HCT-116 addition with RC cells SW-1463, SW-837) as well as normal human cells (HUVECs, RPE-1) following treatment with 3PO. By conducting these assays, my objective was to acquire a deeper understanding of the impacts of 3PO on these different cell types and shed light on its potential therapeutic implications in CRC treatment.

First, for a period of 96h, cells were subjected to the xCelligence assay, which performs real-time analysis of cell size, morphology, proliferation, and cell-substrate attachment under different concentrations of 3PO. The results show that CRC cells retained their structural characteristics (cell size, cell-matrix adhesion quality) and proliferation ability at 10 μM 3PO. Higher concentrations of 3PO (25, 50 and 75 μM) remarkably decreased cells proliferation and affected the quality of cell-matrix attachment ($P < 0.05$) (Figure 4). HUVECs and RPE-1 cells retained their morphological characteristics and proliferative capacity at low concentrations of 3PO (10 μM) and their cell index was reduced at higher concentrations of 3PO (25, 50, 75 μM) (Figure 4).

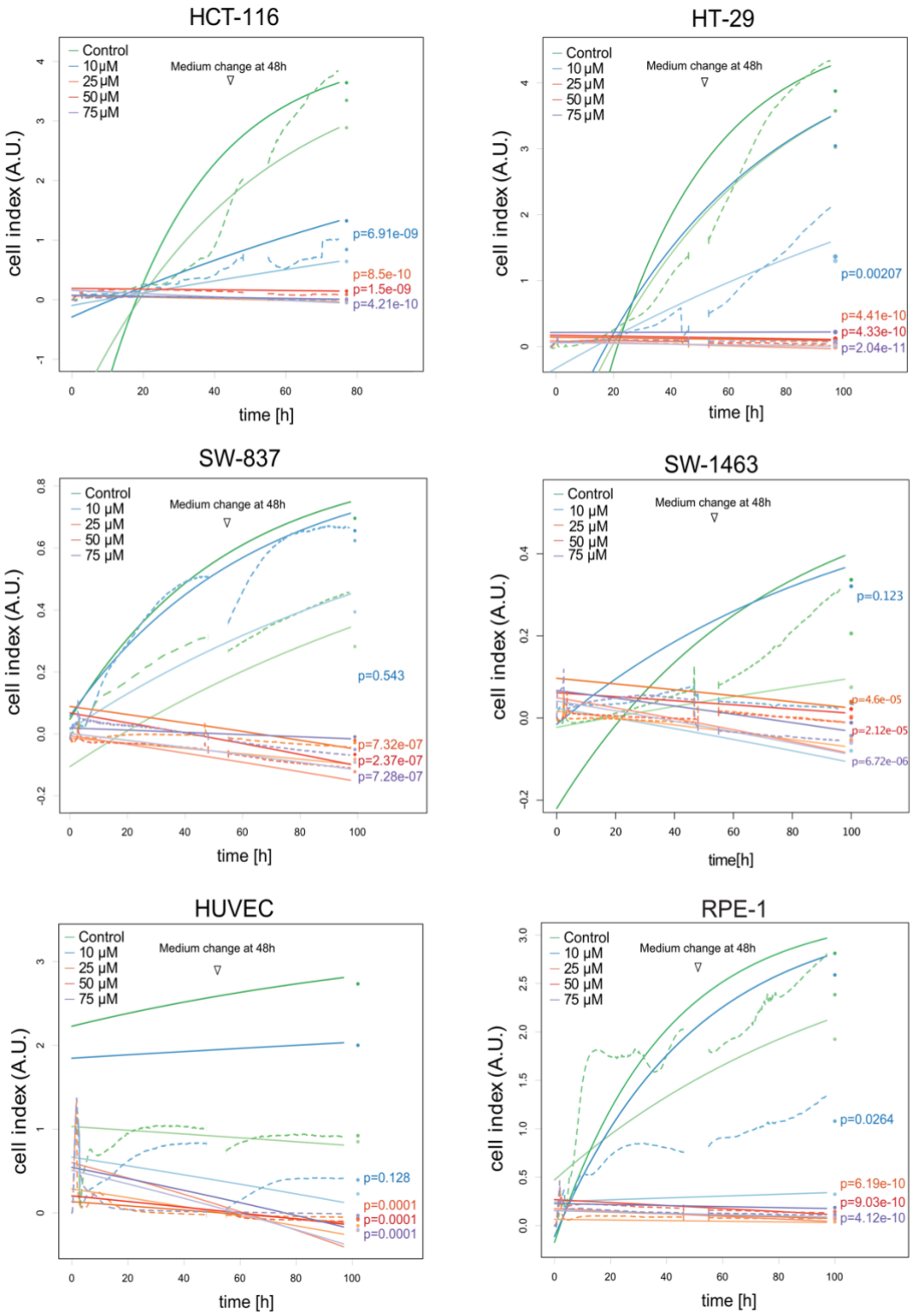

Figure 4. Inhibition of PFKFB3 by the glycolysis inhibitor 3PO reduces CRC cell proliferation in a manner that varies with the concentration. RPE-1, HUVECs, HT-29, HCT-116, SW-1463 and SW-837 cells were detected by xCELLigence assay. RTCA within 96 h at different concentrations of 3PO, dotted lines represent fitted saturation curves, logarithmic, (n = 5).

To delve deeper into the effects of 3PO on cell viability and death, I employed CellTiter Blue and LDH-release assays on both CRC cell lines and non-transformed cells. LDH, a key enzyme in glycolysis, is released into the extracellular environment when there is increased glycolytic activity or a shift towards anaerobic glycolysis. This release of LDH serves as an indicator to assess the intensity of glycolysis and metabolic changes (Muz et al. 2015). Our results demonstrated a clear dose- and time-related reduction in cell viability following 3PO treatment at the 48 h mark (Figure 5A). Consistent with these findings, the release of LDH increased at 48 h marks, indicating that inhibition of glycolysis may enhance cell death (Figure 5B).

Remarkably, the data unveiled that CRC cells were more susceptible to low doses of 3PO (10 μM and 25 μM) than normal HUVEC cells. This observation suggests that 3PO may have a selective impact on cancer cells, potentially making it a promising therapy for CRC. Additionally, I observed that both RC cell lines, SW-1463 and SW-837, exhibited significantly lower cell viability and increased LDH-release compared to HT-29 cells and HCT-116 among the CRC cell lines. Among different CRC cell types, variations in metabolic function or other genetic and molecular determinants may be responsible for the varying response to 3PO, as indicated by these findings.

To comprehensively assess the effectiveness and safety of 3PO, further studies are required. Additionally, our observations regarding the variable response of different CRC cell types to 3PO may have implications for personalized cancer treatment approaches.

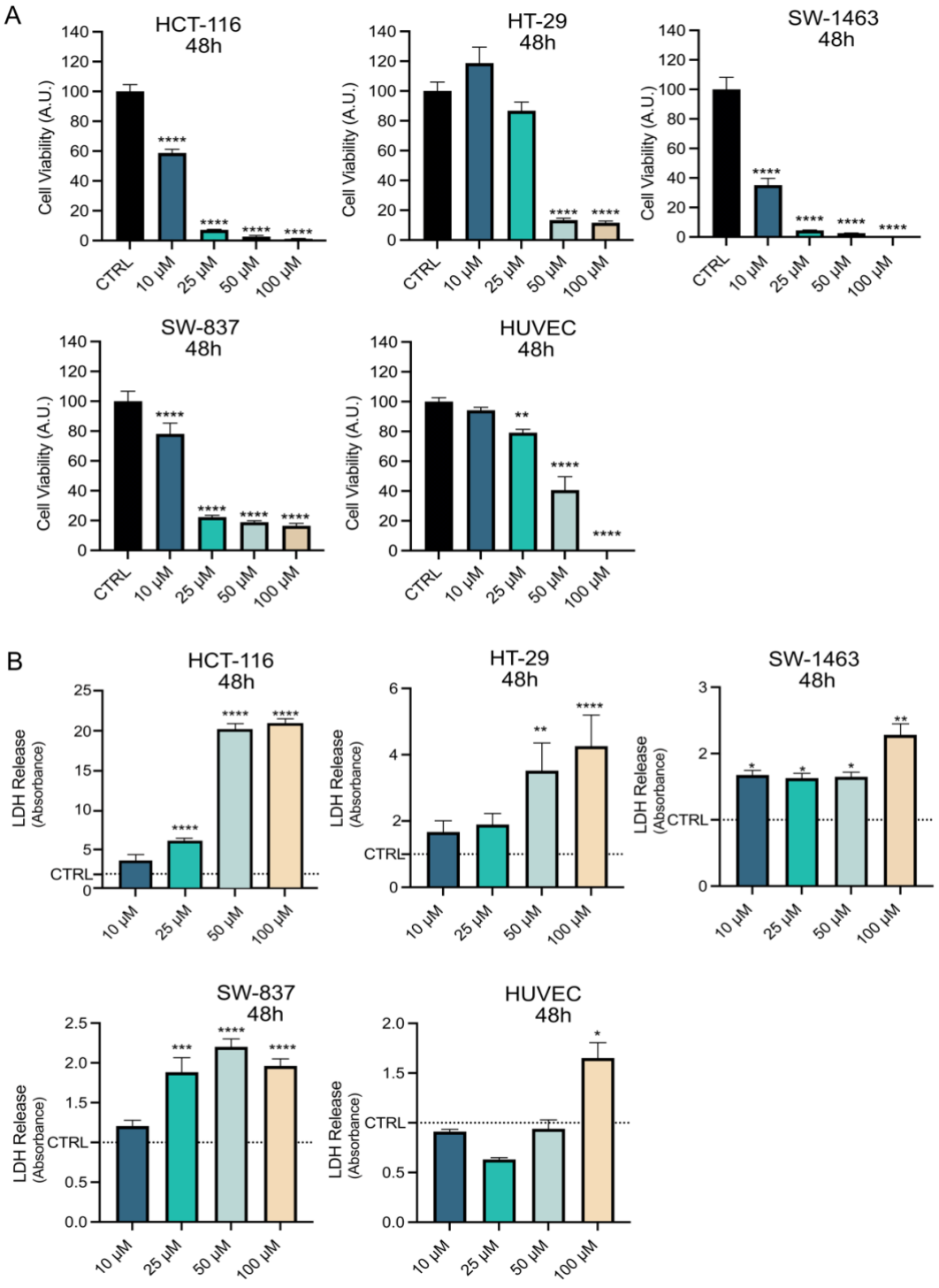

Figure 5. Concentration-dependent induction of cancer cell death by 3PO, a glycolysis inhibitor, through the inhibition of PFKFB3. (A) CellTiter Blue assay was executed using varying concentrations of 3PO on HUVECs, HT-29, HCT-116, SW-837 and SW-1463 cells over a 48 h (n=5). (B) LDH-assay was executed using varying concentrations of 3PO on HUVECs, HT-29, HCT-116, SW-837 and SW-1463 cells over a 48 h (n=5, statistical analysis see Section 2.2.15 for details).

Subsequently, I analyzed a cell counting assay, performed with CC cells HT-29, HCT-116, RC cell line SW-1463 and HUVEC as another independent method for cellular proliferation. After treating these cell lines to varying concentrations of 3PO for 6 h, their respective growth curves were analyzed by counting the cells' number attached to the plate at different time points (Figure 6). The data demonstrate that at 10 µM, 3PO administration did not show any notable alteration on the proliferation rate of all cell lines, growing at a similar rate as the control group (DMSO) (Figure 6). However, the growth rate of the cell lines was markedly diminished after treatment with higher concentrations of 3PO (25 µM), as opposed to the control group. In conclusion, these results reinforce the earlier findings that 3PO effectively reduces CRC cell viability cells in a concentration-dependent manner.

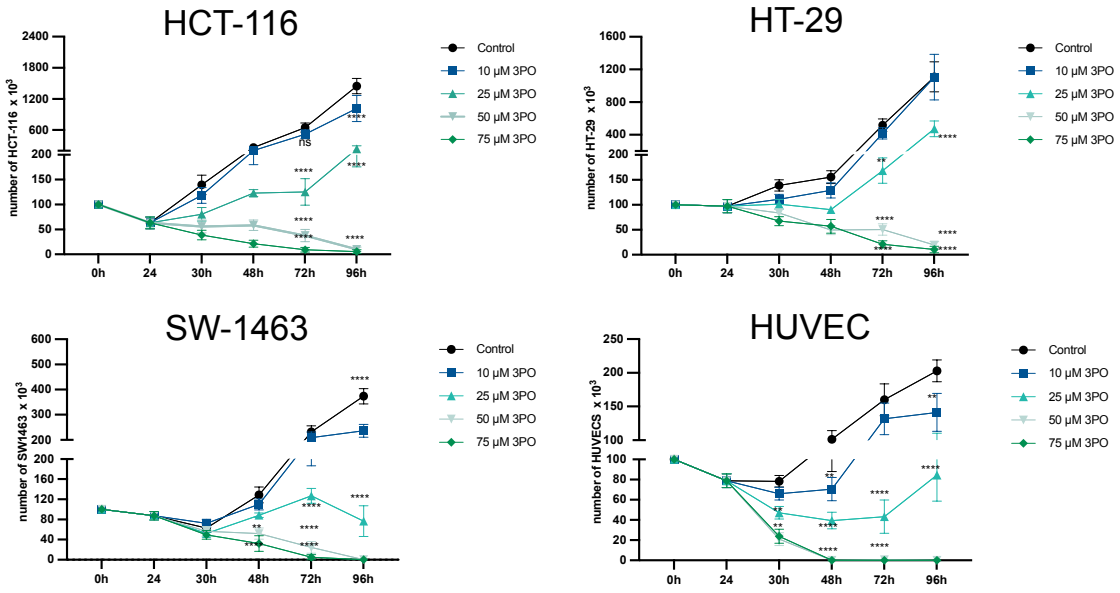

Figure 6. Cell Count assay. CRC cells and ECs cells were exposed to either a low concentration of 3PO (10 µM) or varying high concentrations (25 µM, 50 µM, 75 µM) for a period of 24 h, as indicated on the time scale. Following this exposure, 3PO was washed out. To assess cell growth, cell numbers were counted at specified intervals (n = 5, statistical analysis see Section 2.2.15 for details).

3.2 3PO reduces CRC cell migration, invasiveness and inhibits endothelial sprouting ability

A recent investigation has unveiled that the inhibition of glycolysis via PFKFB3 blockage by the novel glycolytic inhibitor KAN0438757 affects the adhesive properties of CRC cells (De Oliveira et al. 2021). This effect was thought to be related to intracellular structure rearrangement, specifically through the alteration of cytoskeletal components, which is presumed to exert a substantial influence on tumor cell migration and invasion (Seetharaman and Etienne-Manneville 2020).

Building upon these findings and using the xCelligence assay (Figure 4), to investigate the impact of 3PO on invasiveness and motility in CRC cells. Specifically, I conducted scratch assays and Boyden chamber assays to assess CRC invasion and migration in response to 3PO (Figure 7, 8).

I found that while cell migration rates were comparable to the control cells at 10 μM of 3PO treatment, a higher concentration of 3PO (25 μM) significantly reduced the cell migration rate in both HT-29 and SW-837 cells (Figure 7A-D). These findings indicate that the suppression of glycolysis through 3PO treatment might be a potential approach for mitigating CRC cells invade and migrate ability. Additional investigation is justified to uncover the fundamental mechanisms behind this effect and to evaluate the potential clinical utility of this approach.

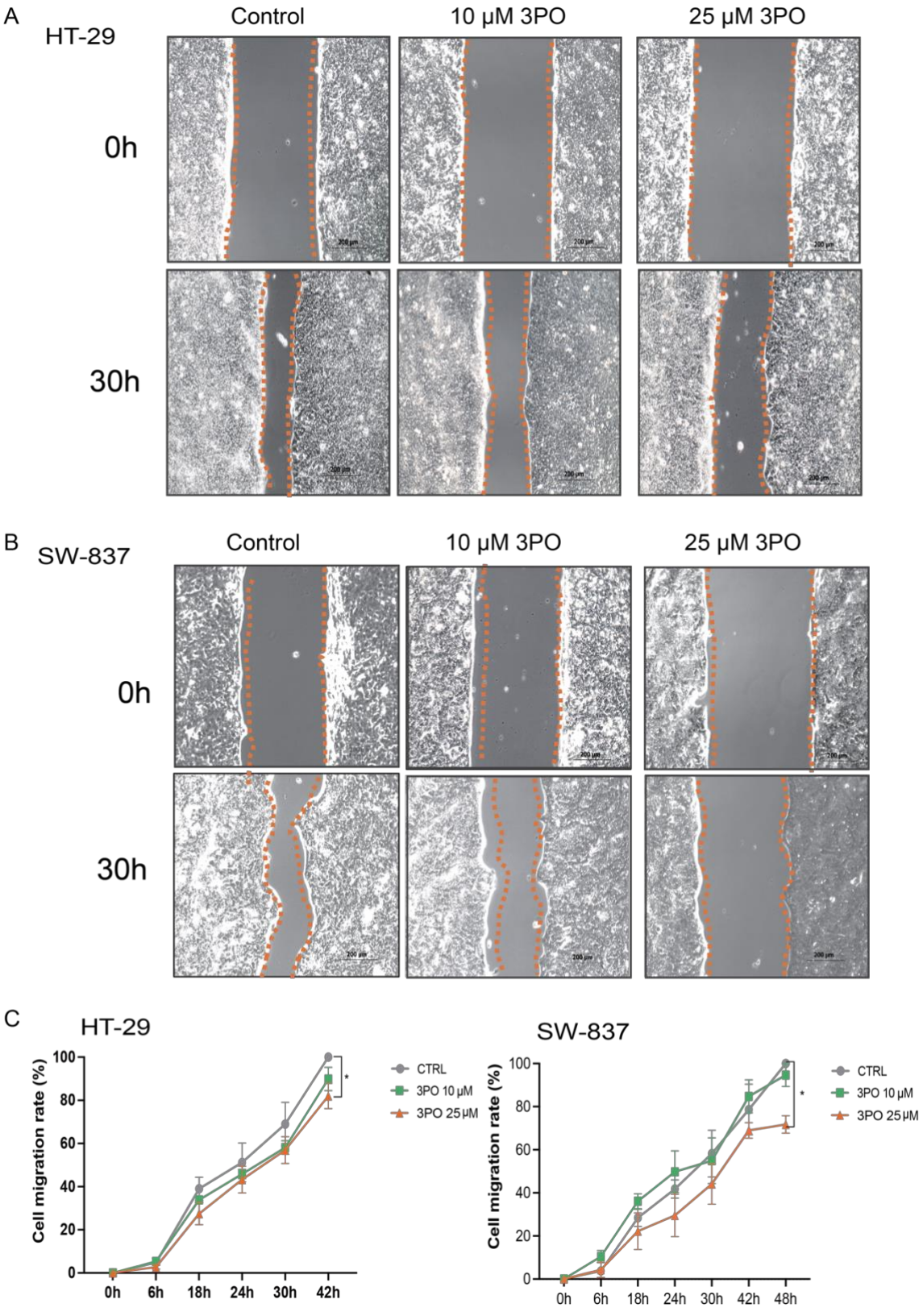

Figure 7. Migration ability of CRC cells was reduced by 3PO. (A-B) Representative images depicting migration assays conducted with HT-29 and SW-837 were subjected to treatment with 25 µM and 10 µM 3PO 0 h and 30 h after removal of IBIDI culture inserts. (C-D) © Quantification of HT-29 and SW-837 cell migration after 42 h and 48 h of treatment with different concentrations of 3PO (n=3, statistical analysis see Section 2.2.15 for details).

To further examine the impacts of 3PO on CRC cells invasion, I conducted a Boyden's chamber assay using four different CRC cells, HCT-116, HT-29, SW-837 and SW-1463. The invasion assay was conducted utilizing a Boyden chamber coated with Cultrex Basement Membrane extract (Path Clear, R&D Systems, MN, USA).

Following a 10 μM concentration 3PO treatment, CRC cells were transferred into Boyden chambers. Collecting lower chamber cells after 96 h of culturing under atmospheric at 37 °C. Our results showed that 3PO treatment (10 μM) for 96 h significantly decrease in the count of invading cells in all the cell lines analyzed (Figure 8).

These findings suggest that PFKFB3 inhibition with 3PO has the capability to decrease CRC cell invasiveness, providing additional evidence for the therapeutic potential of targeting glycolysis in cancer treatment. These results, as illustrated in Figure 8, have important implications for the advancement of innovative therapeutic approaches that inhibit glycolytic metabolism in CRC. To assess the appropriateness and effectiveness of 3PO in both preclinical and clinical contexts, a thorough examination of the molecular mechanisms underlying these effects is warranted through further research.

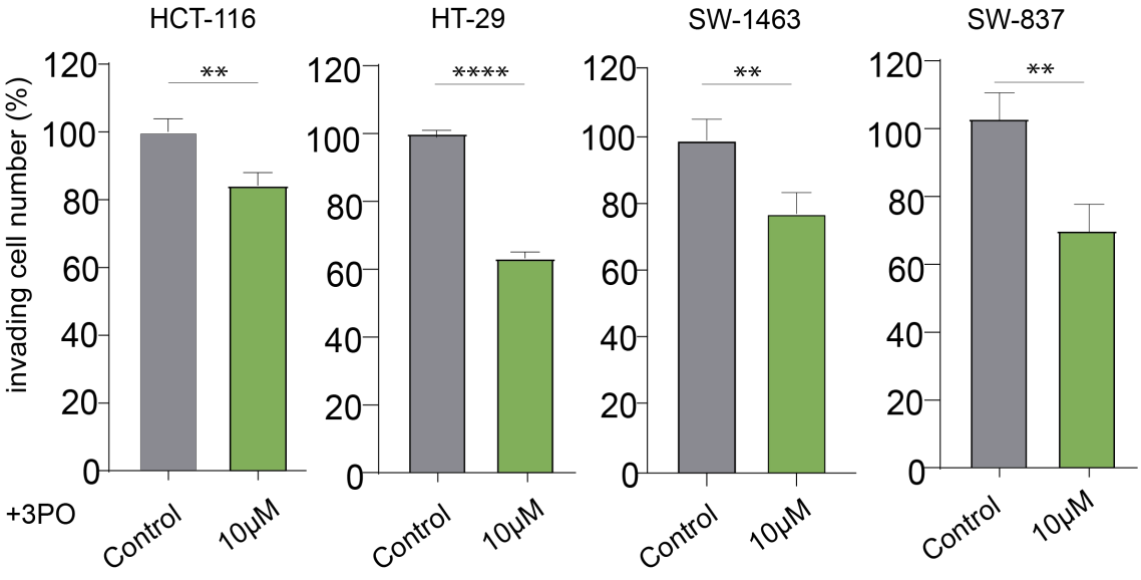

Figure 8. Invasion capabilities of CC cells were reduced by 3PO. Boyden chamber assay results with CRC cells SW-1463, SW-837, HT-29 and HCT-116 to 10 μM of 3PO for a duration of 96 h (n=2, statistical analysis see Section 2.2.15 for details).

Prior research has shown that by inhibiting PFKFB3, the endocytosis of VE-cadherin in ECs was reduced, resulting in a tightened vascular barrier, leading to increased quiescence and adhesion of pericytes. These effects promoted TVN, improved vascular maturation, perfusion and decreased cancer cell migration, endocytosis and metastasis (Cantelmo A. R. et al. 2016). To further evaluate the impact of the 3PO on vascularity, I conducted endothelial sprouting experiments using HUVECs (Figure 9A).

To form spheroids, HUVECs were mixed with ECGM2 and 2 % methylcellulose overnight and fibrinogen and thrombin were added for solidification. The spheroids were then subjected to treatment with either DMSO or 3PO for 24 h (Figure 9A). *In vitro*, angiogenesis was assessed by quantifying sprout length and the count of vessel-like structures.

Our results showed that 3PO treatment at a concentration of 20 μM notably decreased the sprout, while also leading to a diminished count of vessel-like structures (Figure 9B). These findings suggest that PFKFB3 inhibition with 3PO may have a potential therapeutic effect on angiogenesis in CRC. This is a process closely linked to tumor growth and metastasis.

One possible mechanism can account for these observations: PFKFB3 inhibition results in the upregulation of VE-cadherin levels on the plasma membrane, consequently inducing a tighter endothelial cell barrier and inhibits the endocytosis of cancer cells (Cantelmo A. R. et al. 2016; Mazzone et al. 2009). Nevertheless, deeper investigations are necessary to figure out the fundamental processes of 3PO on angiogenesis and to evaluate its clinical potential in the context of CRC treatment. Nonetheless, these findings offer crucial insights into the promise of PFKFB3 inhibitors therapy in CRC treatment and highlight the need for further investigation in this area.

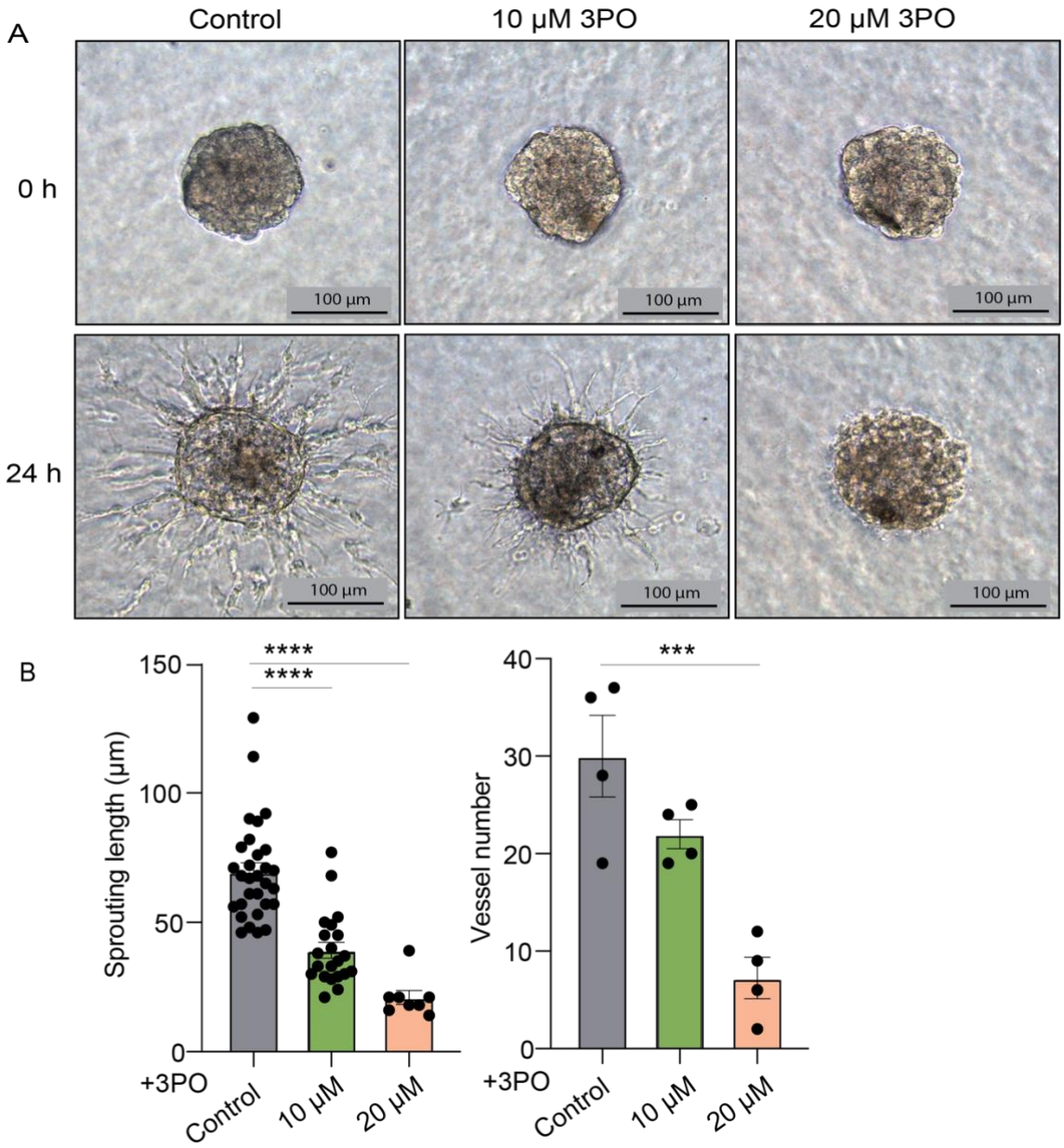

Figure 9. 3PO effects on endothelial sprouting and vessel-like formations. (A)Representative images of endothelial cell sprouting assays performed on HUEVCs exposed to 20 µM and 10 µM 3PO after 0 h and 24 h. (B) Quantification of sprout length and the count of vessel-like structures were analyzed 24 h after exposure to 10 µM and 20 µM 3PO (n=3, statistical analysis see Section 2.2.15 for details).

PFKFB3, as previously discussed, exerts a critical influence on tumor cell glycolytic metabolism, influencing cell invasion and apoptosis (De Bock et al. 2013; Warburg 1956). Given that 3PO acts as an inhibitor of PFKFB3, it is anticipated to have an impact on the conduct of cancerous cells. Thus, I hypothesized that a reduction in germination observed in the sphere experiment (Figure 9A, B) could be ascribed to the compromised proliferation of tumor ECs. To investigate this conjecture, I employed the Ki67 protein marker, which is commonly associated with cellular proliferation. To investigate the mechanism behind the inhibitory impact of 3PO on the vascular sprouting of ECs, I performed Ki67 staining on endothelial cell spheroids that were treated with 3PO (Figure 10A). The results were consistent with the findings (Figure 9B), indicating that 3PO treatment markedly decreased the proliferation of ECs, as indicated by a notable decrease in the immunohistochemical staining of Ki67 (Figure 10B). These data implies that 3PO might achieve its inhibitory effect on vascular sprouting by suppressing endothelial cell proliferation, which is an essential process in angiogenesis.

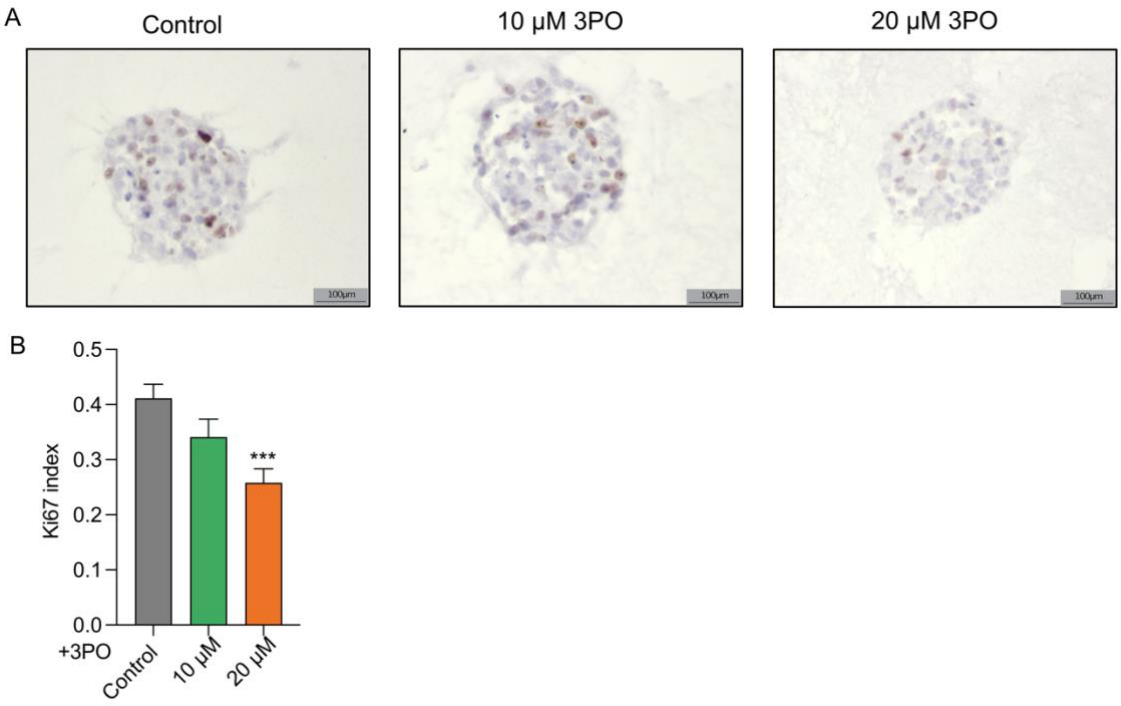

Figure 10. Proliferation evaluation of endothelial sprouting under 3PO treatment. (A) Sprouting assay quantification of HUVECs upon PFKFB3 inhibition. Sprouting EC proliferation was analyzed upon treatment with 20 µM and 10 µM 3PO in 24 h. (B) Representative immunohistochemistry (IHC) pictures from Ki67 positive EC in spheroids (n=3, statistical analysis see Section 2.2.15 for details).

Further investigating the findings presented by Kim (Kim S et al. 2016), which proposed that 3PO only prevents sprout initiation but does not cause the regression of established vascular networks, I decided to evaluate the effects of 3PO on well-established endothelial sprouts (Figure 11A). Following the establishment and 24 h cultivation of endothelial cell spheroids, a subsequent 24 h cultivation was carried out with the administration of 3PO (10 μM, 20μM). Interestingly, I found a reduction in the length of the sprouts (Figure 11B), which contradicts the findings of Kim S. and colleagues (Kim S et al. 2016). This highlights the influence of the experimental model on the obtained data. Thus, my results suggest that 3PO does influence *in vitro* stablished vascular networks.

The study was conducted by ethical guidelines and relevant regulations. Under sterile conditions, treatments were conducted while endothelial sprouts were prepared by culturing ECs on a matrix gel. The length of the sprouts was measured by ImageJ 1.53a and the results were analyzed statistically.

Our experiment provides additional evidence that 3PO may have an anti-angiogenic effect on established blood vessels. Continued study is necessary to fully elucidate the mechanism by which this potential therapeutic agent operates and to assess its potential clinical applications related to angiogenesis-associated diseases.

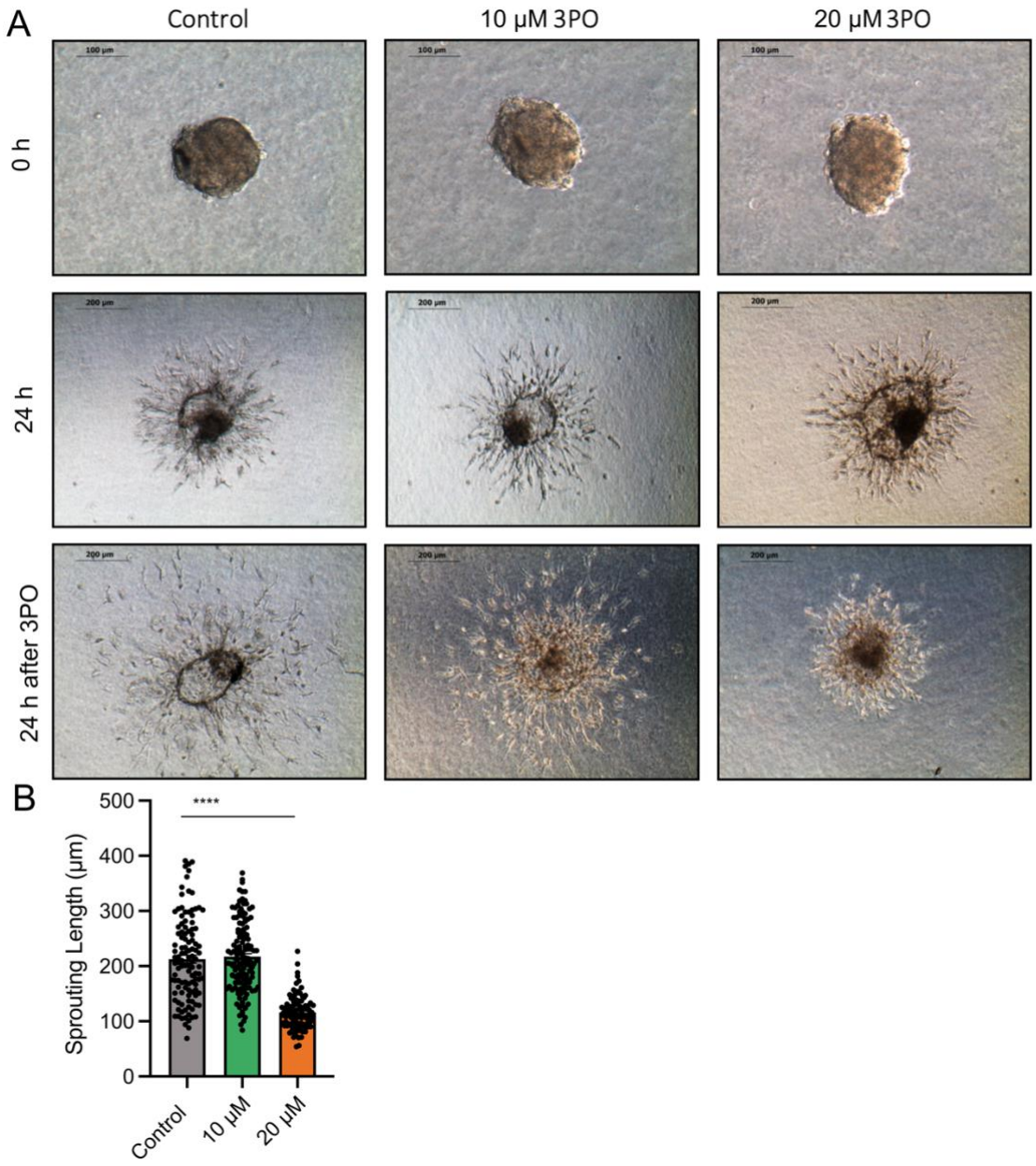

Figure 11. 3PO effects on well-established endothelial sprouting. (A) The endothelial cell HUVECs sprouting was performed following 24 h of incubation, then exposed to 20 µM and 10 µM of 3PO for an additional 24 h. (B) Sprouting length quantification upon 24 h 3PO treatment on already established spheroids (n=3, statistical analysis see Section 2.2.15 for details).

3.3 3PO improves RT induced impairment of CRC cell viability

Cancer cells are known to predominantly depending on glycolysis for their energy needs, which is essential for their continual growth (Lincet and Icard 2015). PFKFB3 as a key regulator of glycolysis, exhibits significant upregulation in CRC (De Oliveira et al. 2021). As previously shown, inhibition of PFKFB3 expression can inhibit the viability of CRC and has been shown to cause cytotoxic effects. Given this knowledge, I have formulated a hypothesis that high expression of PFKFB3 could increase the chemo- and radio-resistance of CRC. Consequently, I conducted CTB experiments to explore the impact of the synergy between RT and 3PO on CRC cell's ability.

When CRC cells were concurrently treated with RT and 3PO, our results revealed a noteworthy decrease in their viability, as opposed to treatment with RT alone (Figure 12). Notably, the SW-1463 and HT-29 cells subjected to RT alone displayed a rise in cell viability after 48 h, as opposed to the control group, indicating the negative impact of RT treatment alone, as previously documented in scientific publication (Wang J-S et al. 2018).

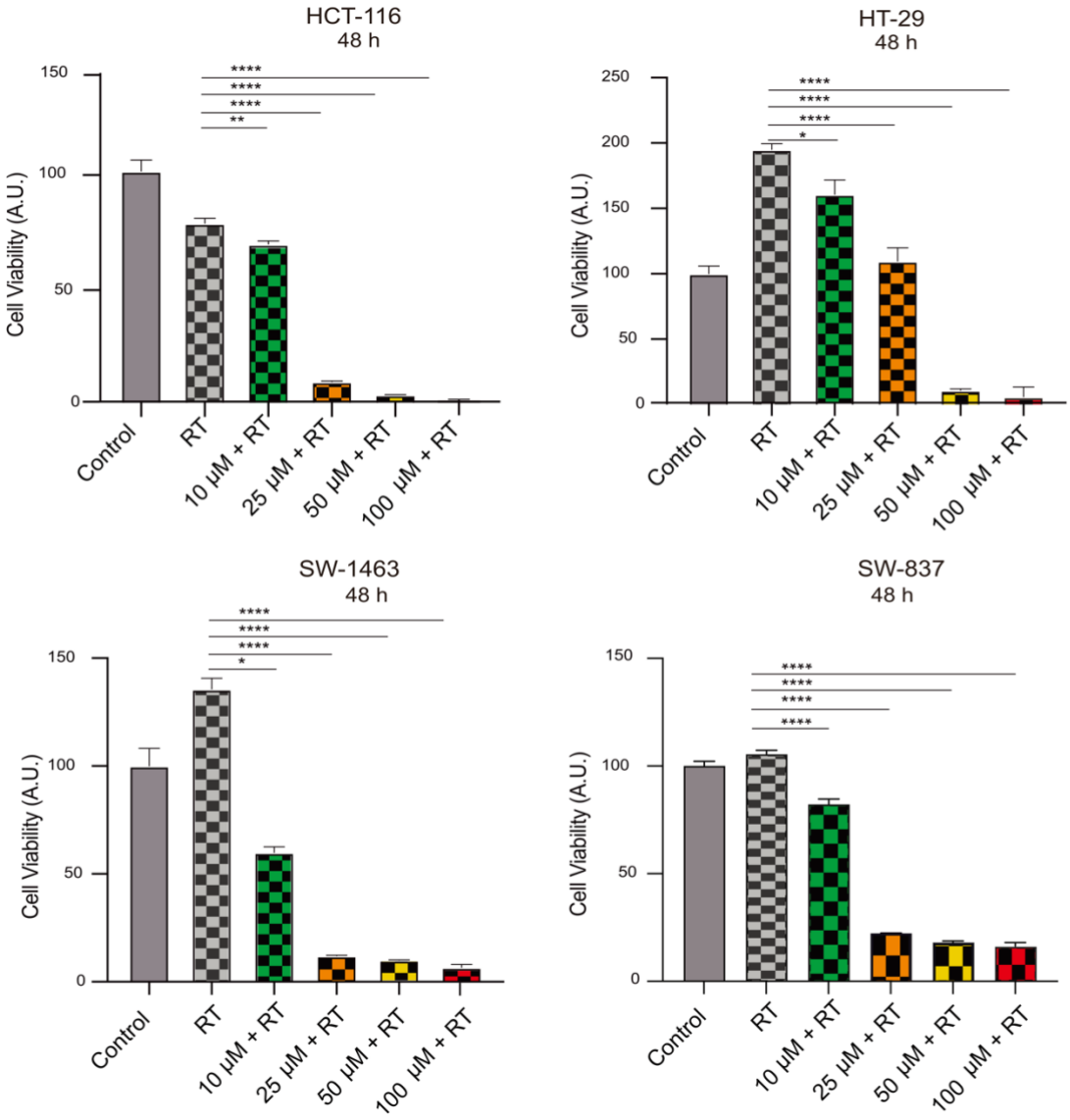

Figure 12. The viability of CRC cells is affected by the combined action of 3PO and RT. CTB was performed on HT-29, HCT-116, SW-1463 and SW-837 cells that treatment with 3PO and RT had lasted for 48 h. Different concentrations of 3PO were administered for 4 h, followed by exposure to RT (6 Gy) and the analysis was performed 48 h later using a fluorescence microplate reader (n=6, statistical analysis see Section 2.2.15 for details).

To augment the findings of the CTB, I conducted further investigations on cell death in CRC cells exposed to a combination of 3PO and RT. Our results from both LDH and CTB assays are concordant with each other. Specifically, in the group treated with 3PO combined with RT, the release of CRC cytotoxicity was higher than in the RT and comparison groups (Figure 13). This evidence strongly suggests that 3PO can enhance the efficacy of RT for CRC.

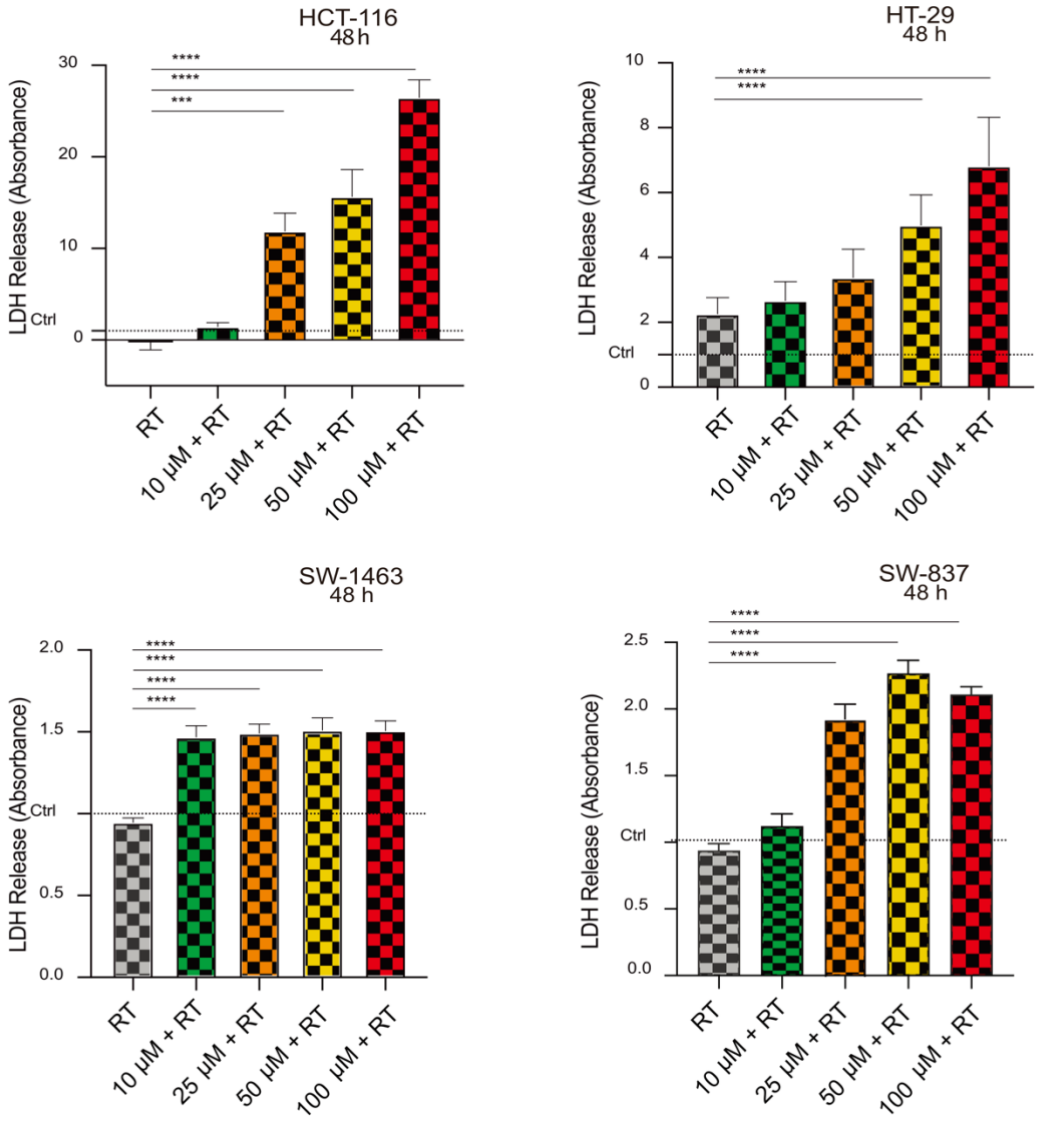

Figure 13. Synergistic effects of 3PO and RT on CRC cell death. The LDH assay was conducted using HT-29, HCT-116, SW-1463 and SW-837 treated with 3PO and RT for 48 h. The CRC cells were exposed to different doses of 3PO for 4 h, then exposure to 6 Gy of RT and analyzed after 48 h using a fluorescence microplate reader (n=6, statistical analysis see Section 2.2.15 for details).

The colony assay represents the gold standard for evaluating cellular demise after IR exposure. It is also a valuable tool for assessing the effectiveness of cytotoxic agents and for investigating drug–IR interactions (Franken et al. 2006). To present a more complete analysis of the impact of combining RT with 3PO, I conducted additional analyses of the clonogenic behavior.

I performed a colony formation assay with all four CRC cell lines and subjected them to combination therapy, consisting of increasing concentrations of 3PO and a single dose of RT (6 Gy). It is noteworthy that due to the stringent requirements of the colony experiment, only a limited number of cells (ranging from 500 to a few thousand) were initially inoculated in each well. Consequently, the concentration of 3PO had to be adjusted accordingly to ensure the viability of the cells and avoid any confounding effects on the experimental outcome. Quantification of the cells' survival fraction showed that all CRC cell lines exhibited a significant decrease in cell survival upon combination treatment of 3PO and RT compared to 3PO or RT alone (Figure 14), thereby corroborating our earlier findings. Overall, our findings substantiate the hypothesis that 3PO can augment the responsiveness of CRC cells to RT.

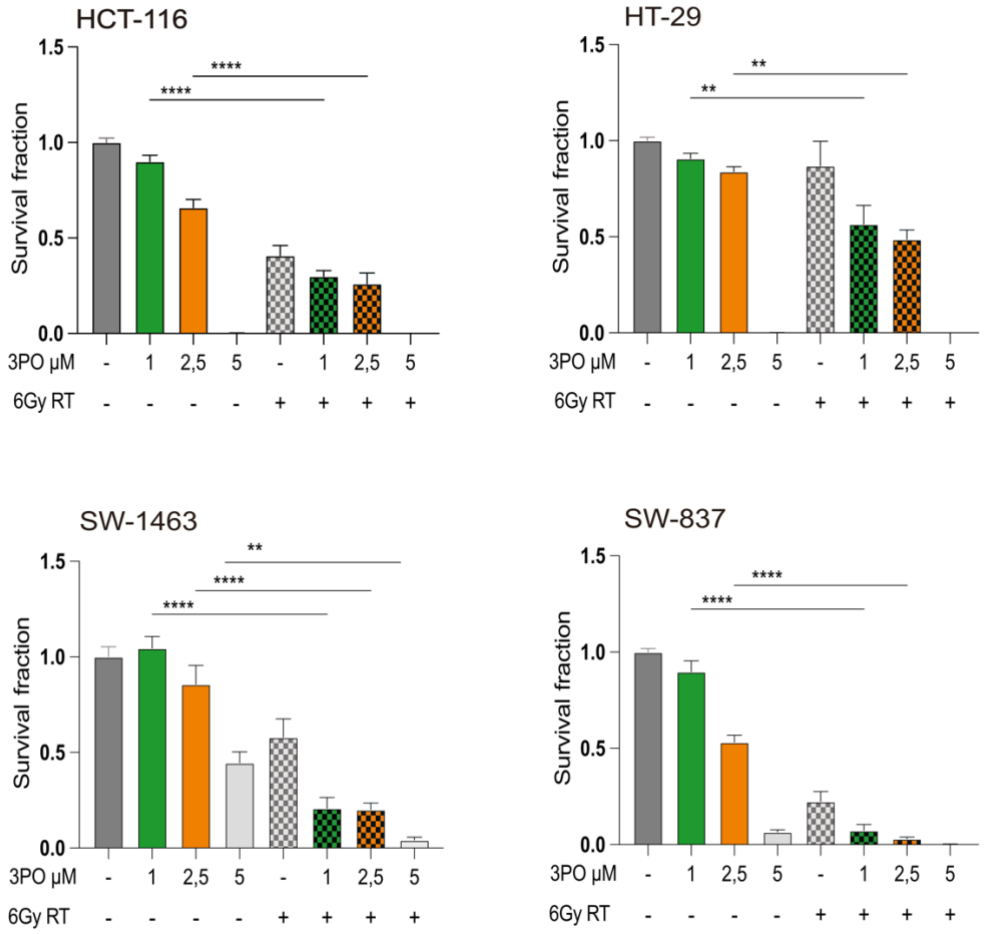

Figure 14. 3PO enhances the effects of RT on colony formation assay. Colony formation assay conducted with HT-29, HCT-116, SW-1463 and SW-837 cell lines treated with various doses of 3PO for 4h, exposed to either RT (6 Gy) or not irradiated and analyzed after 6 days (HCT-116), 7 days (HT-29) and 14 days (SW-1463 and SW-837) by counting colonies (n=8, statistical analysis see Section 2.2.15 for details).

3.4 3PO treatment enriches oxidative phosphorylation gene sets in patient-derived cancer organoids

To understand how 3PO treatments impact cellular processes in a complex *in vitro* model, I utilized previously acquired data from our group on intestinal PDOs.

Organoids are 3D models that mimic the architecture and capabilities of native tissue, typically originating from tissue-specific stem or pluripotent stem cells. These models are advantageous as they provide a closer representation of the *in vivo* physiological conditions, cell-cell interactions and heterogeneity of cell populations compared to traditional 2D cell cultures (Clevers 2016).

In this study, I utilized intestinal PDOs to investigate how 3PO treatment impacts the transcriptome of CC cells. Three CC PDOs were treated by 30 μM 3PO in 24 h. Their RNA was extracted and analyzed by sequencing. Our results indicate that treatment with 3PO did not affect the morphology of the tumor organoids or inhibit their growth during the 24 h experimental period. This suggests that the PDOs remained viable and functional under these conditions, allowing us to evaluate the effect of 3PO treatment influences the cellular transcriptome without any confounding effects from altered cellular viability or morphology (Figure 15A, B).

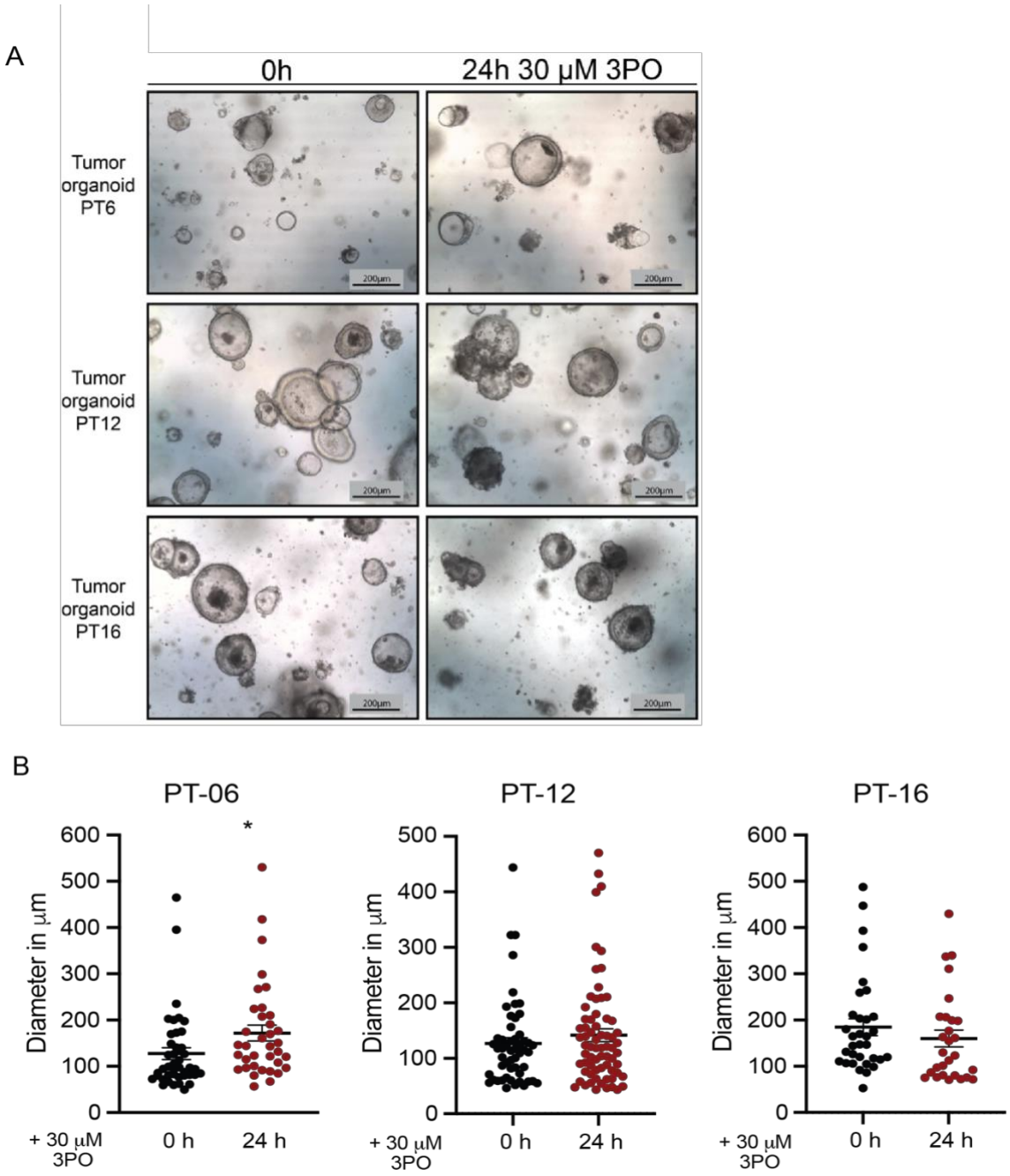

Figure 15. 3PO treatment did not inhibit the growth of PDOs. (A) Scale bars of 200 µm were used to depict representative images of PDOs exposed to 30 µM 3PO for 24 h. (B) Patient-derived tumor organoids' size quantification (n=2, statistical analysis see Section 2.2.15 for details).

Following this, my objective was to assess how 3PO treatment impacts the metabolic status of organoids, whether it would induce a transition to oxidative phosphorylation instead of glycolysis. Therefore, I treated intestinal PDOs with 30 μM of 3PO for 24 h (Figure 15A), following with RNA extraction and bulk RNA sequencing (Figure 16).

The gene expression data obtained were analyzed by GSEA, with the assistance of experts from the Medical Bioinformatics department at the University of Göttingen, Germany, and other colleagues from my research team (Ms. Dorothée Sartorius, AG Conradi, University Medical Center Göttingen, Göttingen, Germany).

We analyzed the resulting gene expression data using GSEA and found that when using the gene set collection "Biological Process" (Ashburner et al. 2000), nine were found to be correlated with oxidative mitochondrial translation and phosphorylation (Figure 16). This supports our hypothesis that 3PO treatment promotes a metabolic transition to oxidative phosphorylation in organoids.

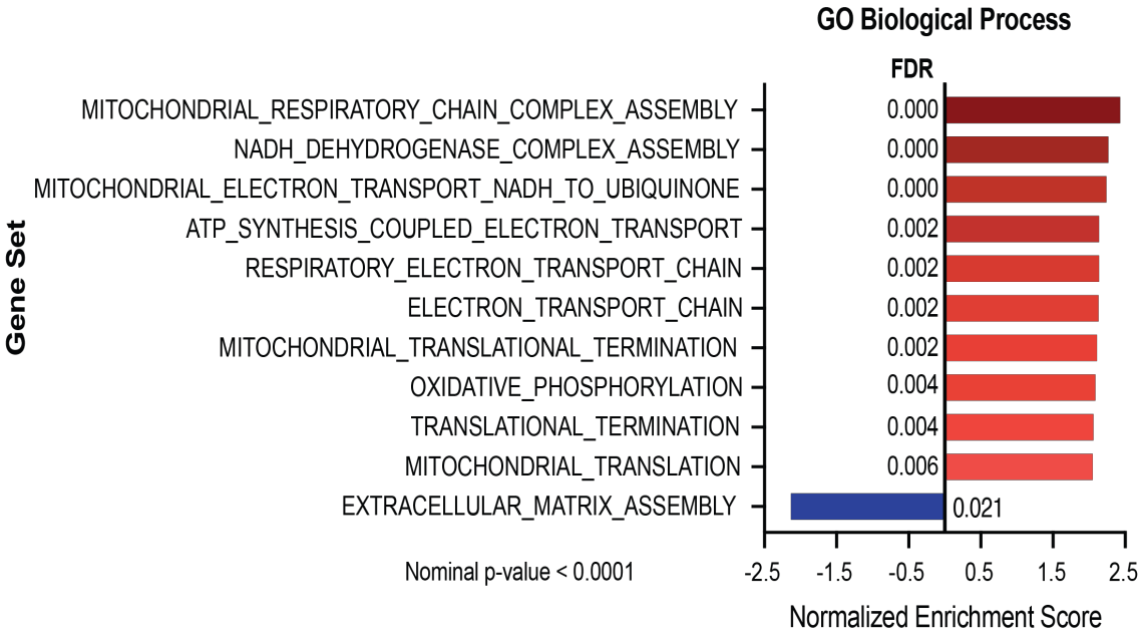

Figure 16. GSEA of 3PO-treated colon organoids to show differences between the phenotypes: tumor control and tumor treated with 30 μM 3PO. Enrichment plots show the running ES alongside the positions of gene set members on the rank-ordered gene list, with genes ranked based on their expression differences between respective classes (rank metric score: signal-to-noise ratio). False discovery rate.

To validate the obtained knowledge about 3PO effects on metabolism and confirm whether the observed transcriptional changes were also observed at the protein level, protein lysates from 3 additional RC organoids were collected, after 24 h of 30 μM 3PO treatment. By immunoblotting analysis, the expression of NDUFB6, ACAD9 and LDHA was evaluated (Figure 17A). The findings revealed that LDHA, a well-established glycolytic marker (Mishra and Banerjee 2019), was downregulated following 3PO treatment in PT-73 and PT-79. This suggests that 3PO treatment may lead to a decrease in glycolytic activity in these cancer organoids. Furthermore, the study identified two proteins linked to oxidative phosphorylation: NDUFB6, and ACAD9, which were upregulated in response to 3PO treatment. NDUFB6 is a subunit of mitochondrial complex I, which performs a critical function in the process of oxidative phosphorylation, ultimately leading to adenosine triphosphate production. (Sharma et al. 2009). ACAD9 is an acyl-CoA dehydrogenase that is involved in energy metabolism and fatty acid oxidation. Studies conducted previously have indicated that ACAD9 expression is decreased in multiple diseases, including CRC, and its downregulation related to an unfavorable clinical outcome (Nouws et al. 2010). The upregulation of NDUFB6 and ACAD9 following 3PO treatment may also contribute to the shift towards oxidative phosphorylation and the inhibition of glycolysis.

Western blot analysis revealed an increase in NDUFB6 expression following 3PO treatment in all four cell lines (Figure 17B). After 3PO treatment, the increased expression of NDUFB6 could potentially alter the energy metabolism of CRC cells, transitioning them from relying on glycolysis towards favoring oxidative phosphorylation, resulting in reduced tumor growth and proliferation. These results suggest that 3PO might be able to modulate PDOs transcription to increase oxidative phosphorylation.

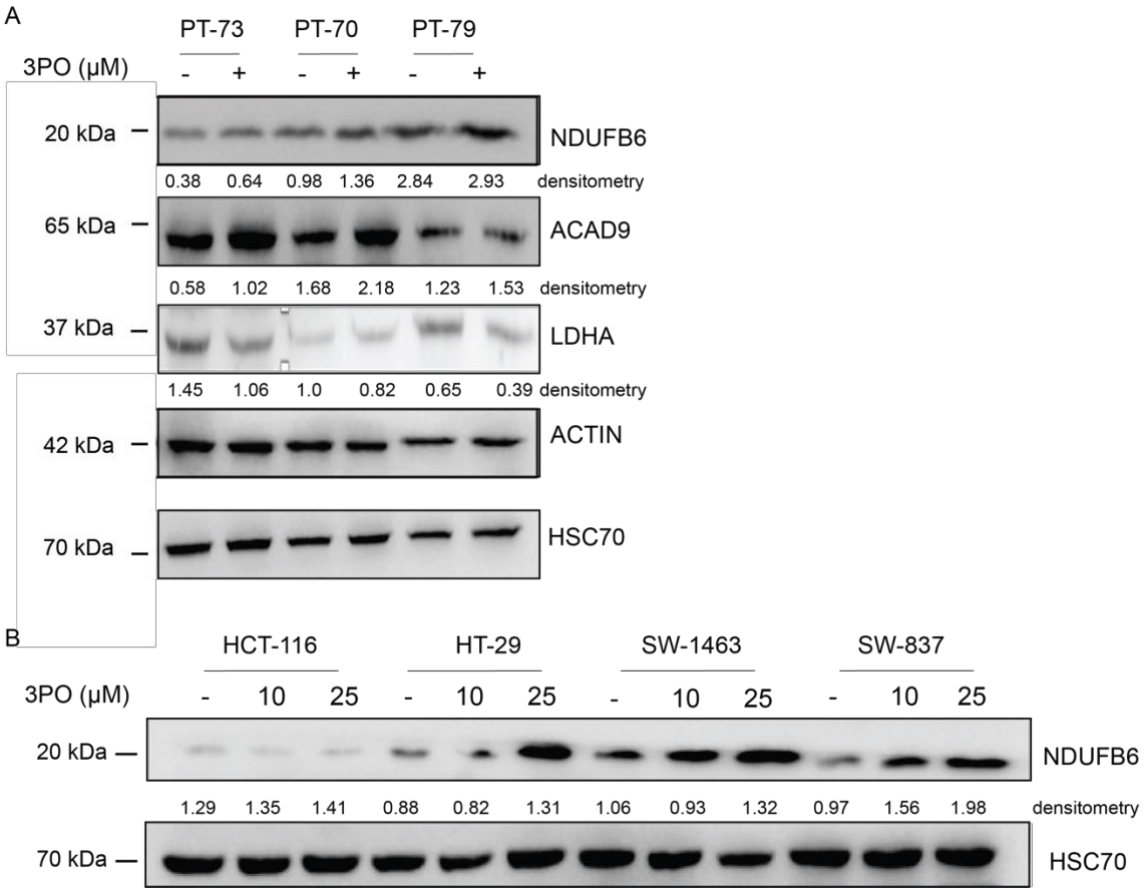

Figure 17. Immunoblot analysis of PDOs and CRC cells' lysates. (A-B) The expression of NDUFB6, ACAD9 and LDHA proteins was assessed in three CRC organoids (PT-73, PT-70 and PT-79), as well as CRC cell lines exposed with 30 μM 3PO for 24 h. Actin and HSC70 were used as loading controls. Images were cropped and analyzed using ImageJ 1.53a software for densitometry.

3.5 Combinatory 3PO and RT treatment induced TVN and increased DNA damage *in vivo*

Our laboratory has previously established a PDX model using RC cell lines to explore *the in vivo* role of 3PO. The experimental setups, results, and analyses are currently under peer-review evaluation (Edelmann M, Fan S, *et al.*, *submitted*). Briefly, to initiate tumor growth, human rectal tumor fragments measuring approximately 2 × 2 mm^3 were implanted into the flank of immunocompromised PrkdcScid mice, following established protocols (Serreze et al. 1995; Shultz et al. 1995). Once the tumors had reached a typical size ranging from 150-200 mm^3, the mice were segregated into four experimental groups: (i) control group, (ii) 3PO 25 mg/kg group, (iii) RT group (14 days; 1.80 Gy/day), and (iv) a combination of 3PO and RT group (Figure 18A, B). Tumor-bearing mice were monitored for changes in tumor size, tumor viability and proliferation (Edelmann M, Fan S, *et al.*, *submitted*).

This *in vivo* experiment primarily sought to estimate the effect of 3PO, RT and the combination of both, in reducing rectal tumor growth in PDX-bearing mice (Edelmann M, Fan S, *et al.*, *submitted*). Now, in the currently work, I aim to further characterize the *in vivo* findings and its underlining molecular mechanisms, involved in the treatment response upon 3PO administration with RT. Therefore, to further investigate the underlying causes involved in tumor response to therapy, I performed TUNEL and cleaved caspase 3 staining with the PDXs tumor sections from all treated animals. Caspase 3 activation stands as a definitive indicator of apoptosis, a programmed cell death process (Porter and Jänicke 1999), while TUNEL staining detects DNA fragmentation (Mirzayans and Murray 2020), another hallmark of apoptosis.

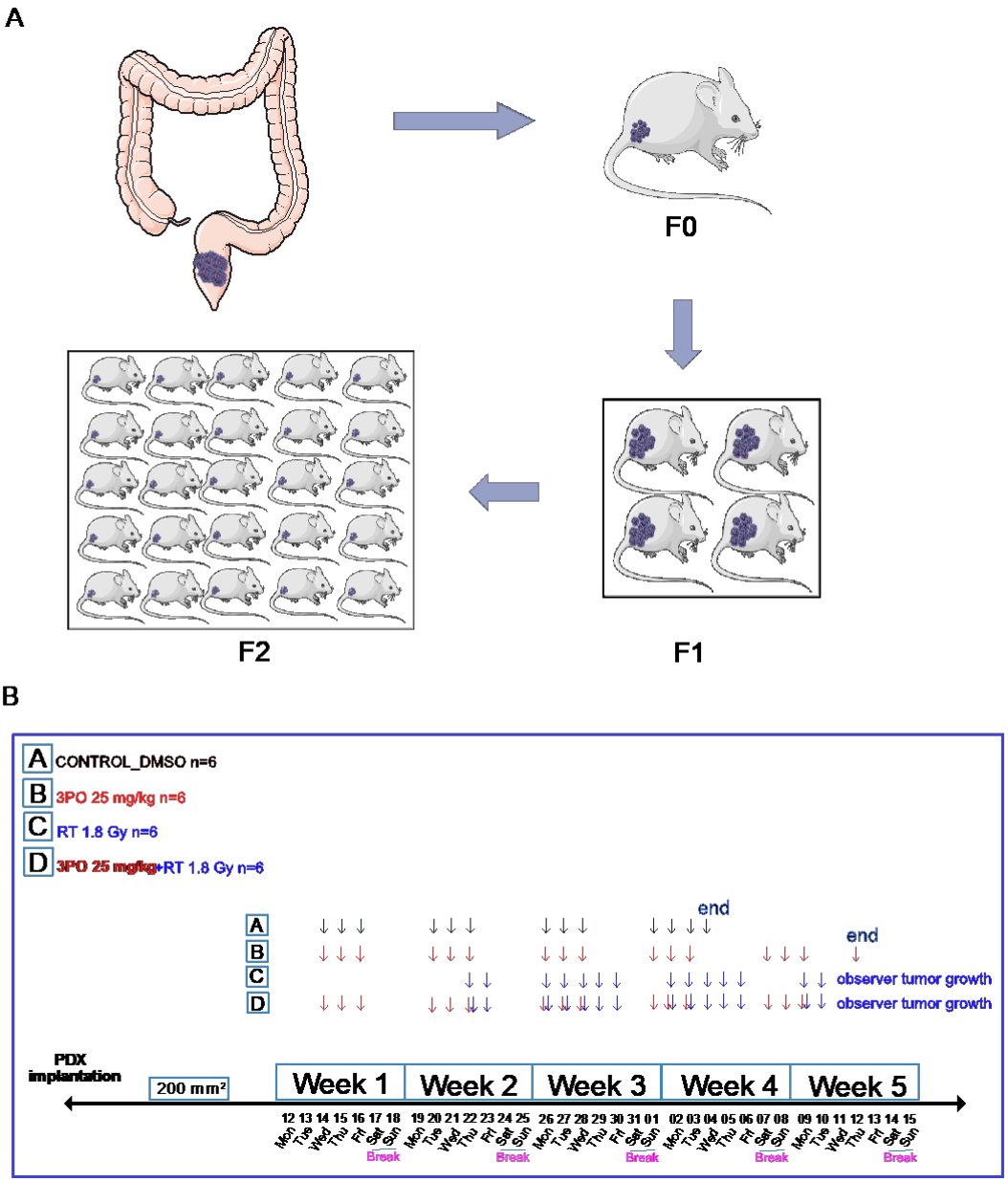

Figure 18. *In vivo* 3PO administration in combination with RT. (A) RC PDX model, fresh-isolated human colorectal tumor samples were transplanted into immunodeficient mice for expansion. (B) PDX growth followed a treatment protocol that simulated clinical conditions, i.e., fractionated radiation doses (14 days; 1.8 Gy/day), in combination with i.p. administration of 25 mg/kg 3PO.

IHC and IF analysis revealed that although the cleaved caspase 3 levels were comparable between single RT group and 3PO + RT combination group (Figure 19A-B), TUNEL-positive cancer cell counts surged in the combination treatment group (Figure 19C-D), suggesting that cell death is not mainly due to increased caspase 3 cleavage (apoptosis). The precise mechanism underlying this effect of 3PO requires further investigation, but it may be related to the modulation of metabolic pathways that regulate cellular energy metabolism and oxidative stress.

In summary, these findings suggest that 3PO treatment results in the induction of apoptosis in CRC cells. Additional research is necessary to clarify the exact processes through which 3PO triggers apoptosis in CRC and to optimize its therapeutic potential.

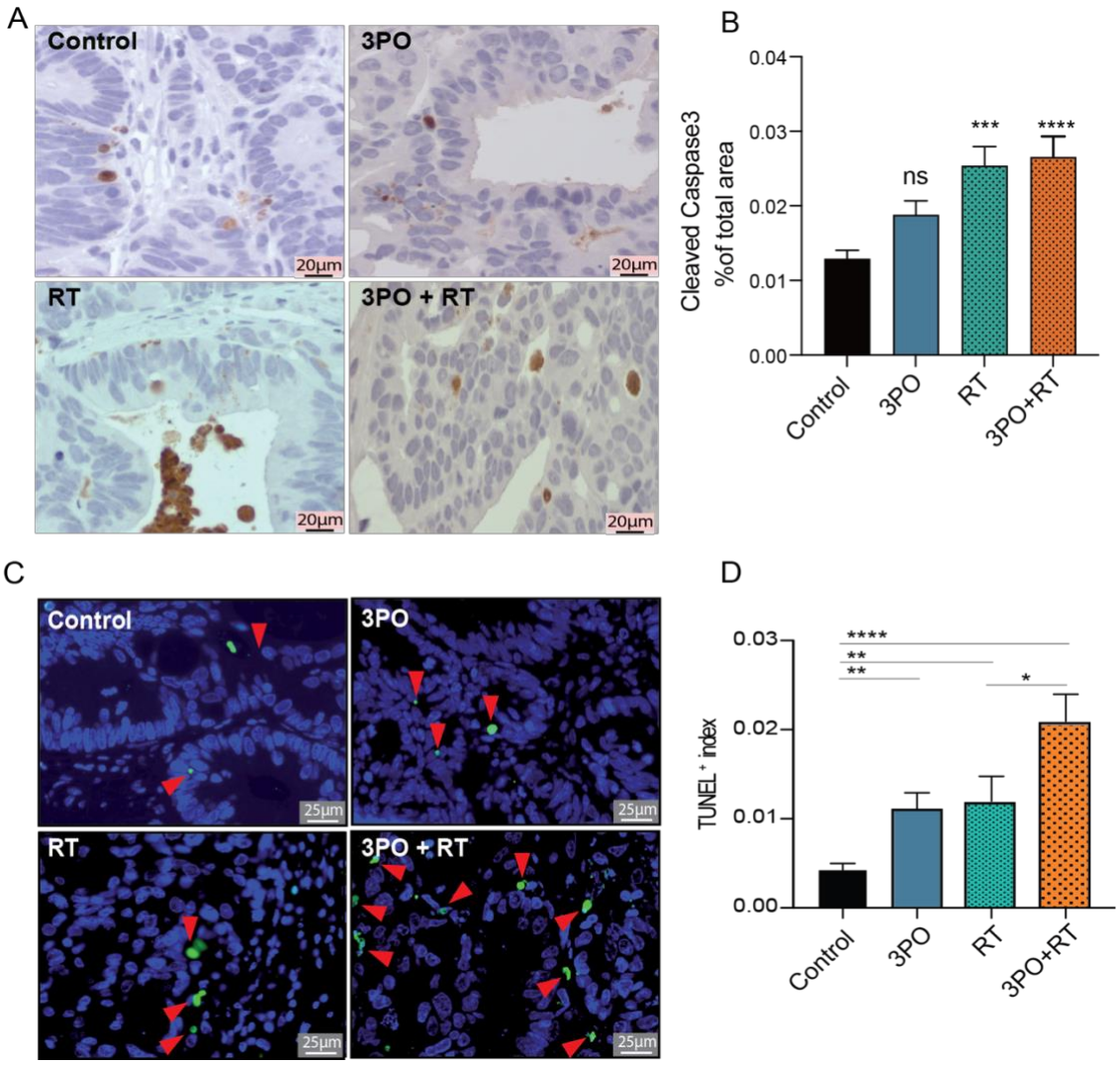

Figure 19. 3PO administration in combination with RT increases tumor necrosis in recatal cancer *in vivo*. (A) Representative micrographs of PDX tumor sections stained for cleaved caspase 3 from control, 3PO, RT and 3PO+RT treated mice. (B) Quantifying apoptosis through cleaved caspase 3 immunostaining (n=4). (C) Representative image of the TUNEL staining in PDX tumors treated with vehicle (Control), 3PO, RT and 3PO+RT. Scale bars, 25 µm. (D) Analysis of DNA fragmentation using TUNEL staining (n=4, tatistical analysis see Section 2.2.15 for details).

To investigate the impact of 3PO administration in conjunction with RT on tumor vascularization, we conducted a co-staining analysis in our PDX tumor samples. Specifically, I used IF staining to detect the expression of two key markers: a vascular marker, cluster of differentiation 31 (CD31) and a pericyte marker αSMA. The results of this co-staining analysis allowed us to establish a definitive link between 3PO administration and changes in tumor vascularization (Figure 20). In comparison to the sham treatment group, tumors treated with RT alone demonstrated a statistically significant reduction in the co-stained CD31+-αSMA+ area, which is indicative of a decrease in vessel density. However, this reduction in vessel density was partially restored in tumors that were concomitantly treated with 3PO, ultimately leading to vessel density that was comparable to that of the sham treatment group.

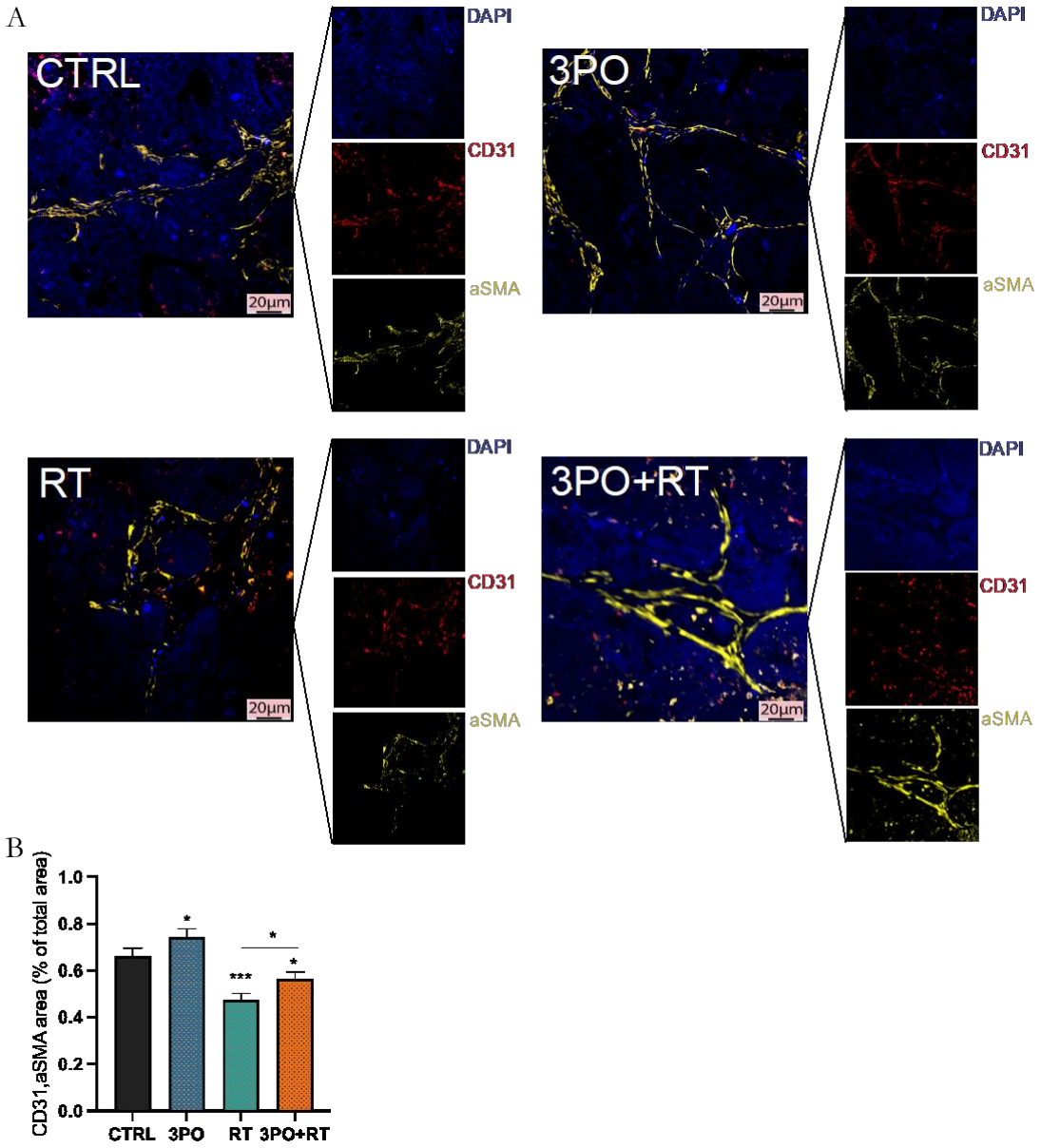

Figure 20. *In vivo,* 3PO administration in combination with RT induces TVN in RC (A) Representative images of CD31$^+$αSMA$^+$ co-stained sections of PDX tumors upon treatment with vehicle (control), 3PO, RT and 3PO+RT. Scale bars, 20 µm. (B) Quantifying the CD31$^+$ αSMA$^+$ area (%), vessel lumen size (µm^2) and tumor vessel number in PDX tumors from control, 3PO, RT, and 3PO+RT-treated mice (n=4, statistical analysis see Section 2.2.15 for details).

To further investigate the impact of 3PO on TVN and its potential association with reactive ROS-mediated DNA damage in human RC patients (Edelmann M, Fan S, *et al.*, *submitted*)), we conducted IHC staining for γ-H2AX (Figure 21A), a marker for DNA double-strand breaks. The aim was to examine whether the increase in tumor oxygenation induced by 3PO treatment would increasing the extent of DNA damage in RC cells.

Analysis of IHC staining revealed an augmented γ-H2AX index in the combined treatment arm of 3PO and RT, indicating increased DNA damage (Figure 21B). These results confirm that the combination of 3PO and RT can effectively trigger TVN *in vivo*, increase ROS-mediated DNA damage and induce cancer cell death.

Additionally, these results indicate the combination of 3PO and RT has the potential to augment the effectiveness of treatment for RC patients by increasing tumor oxygenation, inducing TVN and enhancing ROS-mediated DNA damage. Further research in this area may contribute to the advancement of more potent therapy strategies for RC patients.

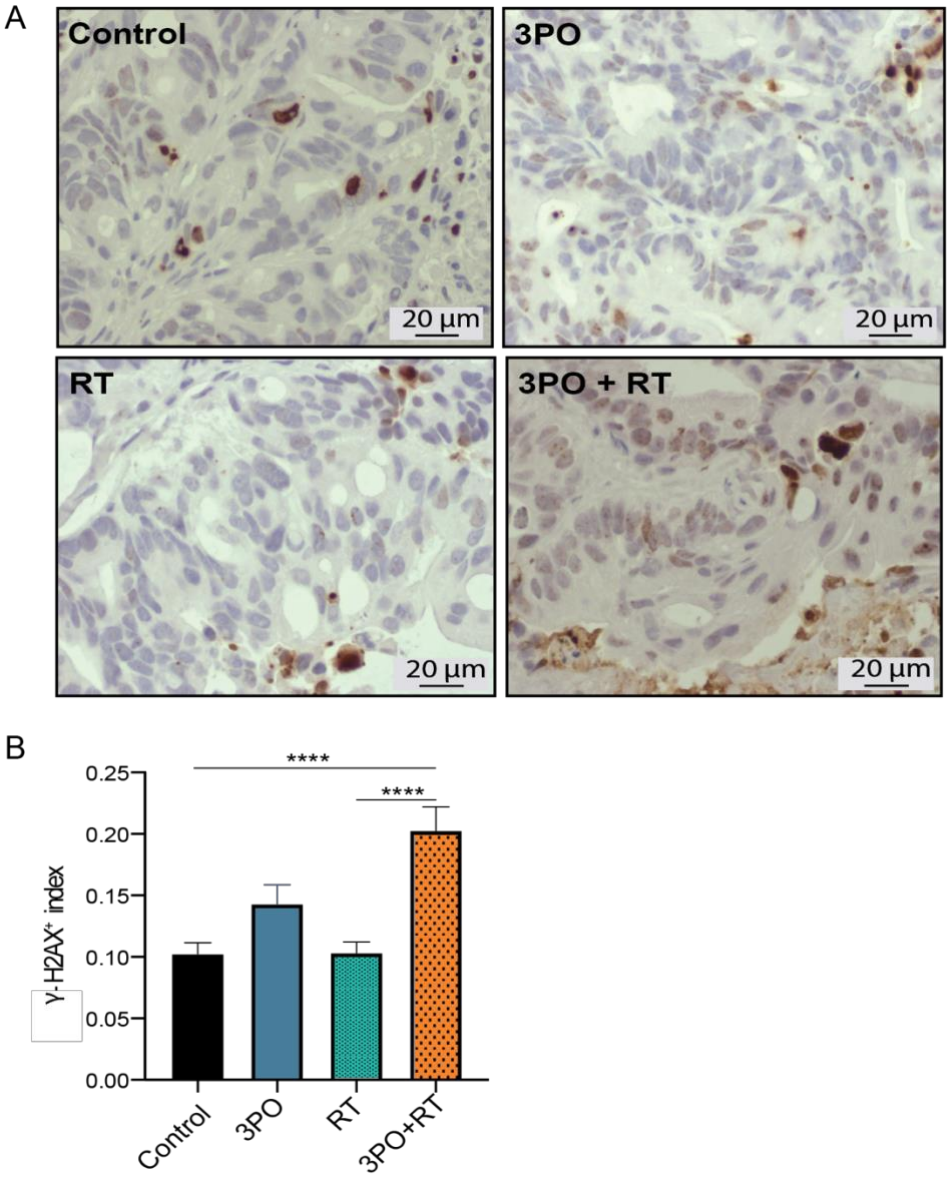

Figure 21. 3PO in combination with RT-enhanced DNA damage *in vivo*. (A) Images of tumor stained with γ-H2AX and taken from PDX tumors in control, 3PO, RT and 3PO+RT-treated mice. The assessment of DNA damage levels was conducted utilizing the γ-H2AX staining. Scale bars, 20 µm. (B) Treated PDX tumors were immunostained and quantified for γ-H2AX (n=4, statistical analysis see Section 2.2.15 for details).

4 Discussion

Worldwide, CRC is the third most widespread cancer (Dekker et al. 2019). Available treatment options for CRC have made significant progress in patients' outcomes in the last decades, but nevertheless, it ranks as the second most influential factor in cancer-related fatalities globally (Bray et al. 2018). For diagnosed with resectable RC in the middle and lower thirds, preoperative short-course RT has demonstrated its efficacy as a therapeutic strategy (Sebag-Montefiore et al. 2009). Despite its beneficial effect in reducing the likelihood of local recurrence, short-term RT administered before surgery does not enhance the overall survival in these patients (van Gijn et al. 2011). According to this, more effective treatments need to be devised urgently.

Currently, neoadjuvant CRT is used in the clinic and has indeed produced positive therapeutic results (Kuipers et al. 2015). Nonetheless, acquired tumor resistance or refractory disease is often observed, necessitating the exploration of alternative treatment strategies (Hammond et al. 2016).

Molecular examination of tumor cells has revealed that, even under aerobic conditions, these cells can depend on glycolysis to generate energy, leading to the production of lactate, the widely acknowledged Warburg phenomenon (Warburg 1956). This metabolic shift is a recognized hallmark of cancer and involves multiple mechanisms (Hanahan Douglas and Weinberg 2011), including alterations in mitochondrial metabolism, upregulation of glucose transporters and dysregulation of signaling pathways associated with glucose metabolism. One key player in this process is the bifunctional enzyme PFKFB3, which is crucial for glucose metabolism (Atsumi et al. 2002).

Elevated PFKFB3 levels in cancer cells stimulates proliferation, migration and apoptosis inhibition (Yalcin et al. 2014). Additionally, PFKFB3 is associated with the regulation of pathological angiogenesis and the promotion of an immunosuppressive TME (De Bock et al. 2013). Within the TME, upregulated CD28-mediated activation of T cell receptor signaling and phosphoinositide 3-kinase-AKT contribute to drug resistance. This metabolic shift promotes the biosynthesis and function of CD8+ and CD4+ cells, impairs the tumor-fighting abilities of natural killer cells and increases lactate production, leading to high acidity in the TME. These alterations suppress immune function and promote tumor progression (Zhong et al. 2022).

This study is to unravel the role of PFKFB3 within endothelial and CRC cells. Prior research has consistently demonstrated that PFKFB3 enhances tumor angiogenesis, proliferation,

migration and apoptosis inhibition (Cantelmo A. R. et al. 2016; Conradi et al. 2017; Yalcin et al. 2014). Given its strong involvement in tumor angiogenesis (Carmeliet and Jain 2011; De Bock et al. 2013), inhibiting PFKFB3 in CRC represents a promising research focus. Therefore, investigating the underlying mechanisms of PFKFB3 inhibition could significantly contribute to CRC treatment (Cantelmo A. R. et al. 2016; Conradi et al. 2017).

By delving into a more profound comprehension of the function of PFKFB3 and its impact on tumor biology, angiogenesis and the immunosuppressive TME, it can identify potential therapeutic targets and strategies for CRC treatment options. The inhibition of PFKFB3 represents an exciting field for further exploration, aiming to addressing therapy resistance and enhancing the overall prognosis of patients with CRC.

4.1 Exploring the effects of 3PO on PFKFB3 inhibition: *in vitro* investigations

The compound 3PO is often employed *in vitro* as an inhibitor of glycolysis and is shown to have inhibitory effects on PFKFB3 (Clem et al. 2008). As previously described, overexpression of PFKFB3 has important effects on the proliferation and metastasis of CRC (Cantelmo A. R. et al. 2016; Conradi et al. 2017).

This investigation delved into how inhibiting PFKFB3 *in vitro* was influenced by 3PO, utilizing ECs, CRC cell line and intestinal PDOs, employing diverse experimental techniques. Initial findings indicate that exposure to 3PO impairs the growth and survival of transformed cell lines, with effects contingent upon both dosage and duration of exposure. This study shows that when lower concentrations of 3PO (10 μM) did not result in noticeable effects on the morphological characteristics or proliferative capacity of CRC cells. However, higher concentrations of 3PO (25, 50, 75 μM) reduced cell proliferation and disrupted cell-matrix attachment. These findings suggest the promise of using 3PO as a treatment option against CRC. Future research could focus on determining the optimal dosage and treatment regimen to maximize its anti-cancer efficacy while minimizing systemic side effects and sparing normal healthy cells.

Moreover, the findings from experiments assessing cell migration and invasion capabilities indicated that 3PO (25 μM) decreased the metastatic and invasive potential of CRC cells. Future studies could focus on investigating the signaling pathways implicated in cell migration, invasion and might offer valuable understanding about the mechanisms that drive the progression of CRC.

Additionally, the reduction in angiogenesis observed in the ECs spheroid assay suggests that 3PO might possess anti-angiogenic properties. Further investigation into the specific mechanisms by which 3PO inhibits angiogenesis might advance the creation of precise treatments for diseases reliant on angiogenesis.

Our *in vitro* model of PDOs assays provided valuable insights into the specific underlying mechanisms in the inhibition of PFKFB3 by 3PO. Notably, we observed a significant metabolic shift from glycolysis to oxidative phosphorylation following treatment with 3PO. This observation suggests that 3PO's therapeutic implications might extend beyond CRC and potentially be applicable to metabolic disorders.

To further evaluate the potential therapeutic applications of 3PO, it would be crucial to assess its effects on cellular metabolism and disease progression using specific disease models. By doing so, it might be possible to enhance our insight into the therapeutic potential of 3PO in various metabolic disorders, broadening its scope beyond CRC.

Moreover, our findings revealed the upregulation of NDUFB6 and ACAD9, markers associated with oxidative phosphorylation, following treatment with 3PO. This upregulation indicates that 3PO might be involved in transcriptional regulation, specifically in modulating the genes express related to oxidative phosphorylation. To unravel the precise molecular mechanisms by which 3PO influences the transcription of these genes, further studies should be conducted.

Taken together, this study demonstrates that 3PO affects the proliferation, metastatic potential, cell-matrix attachment and angiogenesis in CRC cells. Furthermore, in intestinal PDOs, it promotes a metabolic shift towards oxidative phosphorylation. These discoveries offer valuable information regarding the impact of 3PO and its potential as a therapeutic focal point in CRC.

4.2 Addition of 3PO to RT regime increases radiation effects on CRC

Researchers have demonstrated that targeting PFKFB3 increases RT sensitivity and affects the HR (Gustafsson et al. 2018). It has been observed that hyperoxia tumor regions exhibit a better response to RT compared to hypoxic regions (Evans and Koch 2003). Considering that advanced tumors often contain substantial hypoxic areas (Vaupel and Mayer 2007), it is reasonable to speculate that the effects of inhibiting PFKFB3 may be associated with alterations in gene expression that occur during a metabolic shift to oxidative phosphorylation, resulting in a rise in the generation of radiation-triggered ROS. ROS are

highly reactive molecules that capable of inducing harm to DNA and other cellular components, ultimately leading to cell death (Finkel and Holbrook 2000). The metabolic shift induced by inhibiting PFKFB3 may enhance the production of ROS during RT, thereby increasing the effectiveness of treatment. These findings could explain my results obtained with CRC cells, where addition of 3PO to radiation reduced cell's viability.

This mechanism might potentially involve a reduction in the accumulation of glycolytic byproducts such as glutathione and pyruvate, which are essential for facilitating cell proliferation and survival (Gottschalk et al. 2004; Sattler and Mueller-Klieser 2009). Consequently, inhibiting PFKFB3 using a compound like 3PO holds promise as a strategy to enhance the effectiveness of RT in the treatment of CRC. By inhibiting PFKFB3, the metabolic alterations induced by RT, might lead to a decrease in the survival and proliferation signals mediated by glycolytic products, thereby potentially improving the therapeutic effectiveness of RT in case of CRC.

4.3 Effect of 3PO on expression of oxidative phosphorylation-related genes in PDOs

In this investigation, I aim to examine the impacts of 3PO treatment on PDOs specifically focusing on the changes in the activity of oxidative phosphorylation-related genes. The RNA sequencing analysis results indicated significant alteration in the metabolic pathway leading to oxidative phosphorylation in the PDOs (CC) following 3PO treatment (Figure 16). When glycolysis is impaired, as observed in this study, the cells may utilize alternative energy sources such as oxidative phosphorylation to maintain their energy needs (Gottschalk et al. 2004; Lu C-L et al. 2015; Zheng 2012).

Furthermore, I noted a remarkable rise in the expression of NDUFB6 in PDOs (RC) and CRC cells, following 3PO treatment (Figure 17). NDUFB6, a subunit of complex I involved in the generation of energy through oxidative phosphorylation, plays a critical role (Sharma et al. 2009). The observed upregulation of NDUFB6 suggests that 3PO treatment might enhance the activity of complex I, potentially contributing to an increased reliance on oxidative phosphorylation. This finding aligns with earlier research that have reported the absence of complex I results in heightened resistance to RT in CRC, along with an enhanced glycolytic capacity (Shi et al. 2021).

The acquired insights from these results shed light on the fundamental molecular mechanisms involved in the response to 3PO treatment in CC PDOs. Specific genes

involved in oxidative phosphorylation exhibit upregulation, and this is elucidated alongside changes in metabolic pathways, this study provides valuable information that can guide the development of novel therapeutic options for CRC.

Promoting the metabolic reprogramming observed in cancer cells, specifically favoring the shift towards oxidative phosphorylation, could potentially be explored as a strategy to enhance treatment efficacy and overcome therapeutic resistances. Overall, by studying the response of CC PDOs to 3PO treatment, the results offer crucial insights into the associated molecular processes.

4.4 Effectiveness and impact of TVN in RC

Building upon the promising results from my previous *in vitro* and *in vivo* assays exploring the combined effects of 3PO addition to RT on CRC cells, I have chosen to further explore the underlying mechanism of TVN. To accomplish this, I conducted additional investigations using an *in vivo* model of RC PDX.

To assess TVN, I employed IF to evaluate the lumen and density of CD31-stained vessels. My findings revealed a substantial enhancement in the vessel density and the size of the vessel lumen of CD31-stained, indicate progressing in the normalization of tumor blood vessels (Figure 20). This suggests that the combination of 3PO and RT might benefit to the development of functional blood supply to the tumor.

Building upon these findings, I aimed to determine whether the increase in vessel lumen size and vessel density would result in a reduction of hypoxic regions within the tumor. Solid tumors often exhibit hypoxia, which involves low oxygen levels, and this is closely related to CT resistances and unfavorable outcomes (Muz et al. 2015). My findings showed that the addition of 3PO to RT not only decreased hypoxia but also increased γ-H2AX phosphorylation (a marker of DNA damage), suggesting that TVN occurred and triggered reactive ROS-mediated DNA damage (Figure 21). It can be inferred from these findings that this combination treatment not only promotes TVN but also induces DNA damage in cancer cells, potentially leading to their demise.

Based on these observations, this study suggests that 3PO has the capacity to enhance the effectiveness of RT for RC management. The promotion of TVN, reduction of hypoxia, and increased DNA damage, observed with the combined approach of 3PO and RT, could potentially lead to improved therapeutic outcomes for RC patients.

4.5 Limitations of this study and open questions

Although TVN can improve the efficacy of anti-tumor treatment, such as improved drug delivery, enhanced oxygenation, reduction in metastasis and synergistic effects with other CRT, several challenges need to be addressed. One of these challenges is overcoming pharmacological dependence during the induction phase of TVN (Yang et al. 2021).

Maintaining the intricate equilibrium between proangiogenic and antiangiogenic factors in tumor cells is essential for successful TVN. However, the mechanisms underlying this balance and the optimal strategies to manipulate it remain unclear (Cantelmo Anna Rita et al. 2017). Future studies should prioritize unraveling the regulatory pathways and molecular mechanisms involved in regulating proangiogenic and antiangiogenic factors in tumor cells to achieve effective and sustained TVN.

The research conducted in this study was based on targeting the metabolic processes of ECs and blocking the glycolytic process of tumor cells using a PFKFB3 inhibitor. While these findings offer significant insights into the potential of metabolic interventions for TVN, it is essential to determine the generalizability of these findings to other tumor types and therapeutic approaches. Further studies on experimental models for different tumor entities and treatment modalities are necessary to confirm the efficacy of metabolic interventions in inducing TVN in a wider field of tumor entities.

By normalizing the highly unusual function and structure of CRC vessels, enhancing the anti-tumor effect of CRT and reducing the probability of metastasis were the primary goals of this study. However, despite the promising findings of this study, additional inquiries are necessary to elucidate the enduring effects of TVN induction, including its impact on tumor recurrence and the development of resistances to CRT. Additionally, optimizing the dosage and administration schedule of the glycolysis inhibitor, as well as determining the optimal timing and sequencing of TVN induction and CRT, are important factors that require careful consideration in future research endeavors.

In this research, we conducted *in vitro* cell and tissue assays, demonstrating that the use of 3PO significantly ameliorates the impairment of CRC cell viability induced by RT. Furthermore, in our *in vivo* experiments on RC PDXs, we observed that inhibition of PFKFB3 by 3PO resulted in TVN.

However, it is crucial to emphasize that our *in vivo* experiments have only been conducted on RC PDXs. To establish the generalizability and applicability of these findings, further

investigation on CC PDXs is essential. Future studies focusing on CC PDXs will be required to ascertain whether the observed effects remain consistent across different CRC types.

4.6 Outlook

TVN is gaining attention as an additional approach for reducing metastasis and enhancing the effectiveness of CRT and immunotherapy in CRC patients (Carmeliet and Jain 2011; Huang et al. 2013). Inhibiting the activity of PFKFB3 was shown to enhance the effects of standard cytotoxic doses of CT, decreases primary and metastatic tumor growth and inhibits CRC dissemination (Cantelmo A. R. et al. 2016). These results indicate that targeting TECs glycolysis through PFKFB3 inhibition might represent a potential therapeutic strategy of CRC treatment.

Importantly, this work indicates that inhibiting PFKFB3 with the 3PO combination with RT could be reducing CRC cell's survival in *vitro* and might enhance RC treatment effectiveness *in vivo* by inducing TVN. This could ultimately lead to improved clinical outcomes, including higher rates of complete response, when used in combination with existing cancer therapies, such as CT and immunotherapy. These findings emphasize the significance of conducting further investigations on PFKFB3 inhibition as a promising adjunctive therapeutic strategy in CRC treatment, apart from CRT.

5 Abstract

The current treatment approach for CRC involves a combination of surgery and neoadjuvant chemo- and RT. However, drug resistance and recurrence remain significant challenges, emphasizing the need for new and more effective treatments. Recent research has suggested that inhibiting the glycolytic activator PFKFB3 to promote TVN may improve tumor hypoxia and enhance tumor response to therapy. In this research, we performed *in vivo* and *in vitro* assays with PDOs, PDXs and CRC cells to evaluate the impact of 3PO, a PFKFB3 inhibitor on cell survival, clonogenicity, migration, invasion and metabolism. Our findings demonstrate that 3PO enhances radiation-induced CRC cell death, diminishes the metastatic and invasive abilities, and alters the transcriptional metabolism of PDOs, promoting a metabolic shift towards oxidative phosphorylation. Importantly, our results show that 3PO can induce TVN in RC, reducing the tumors' hypoxic environment and enhancing its sensitivity to RT. Collectively, these outcomes point to the conclusion that inhibiting PFKFB3 to facilitate TVN for improve tumor hypoxia, which could represent a compelling new direction for the treatment of CRC. This research might improve to the exploitation of new therapeutic approaches for CRC patients, potentially improving their outcomes.

6 Appendix

Table S1: General laboratory devices

Device	Supplier
Balance (PL602-S)	Mettler-Toledo (Columbus, USA)
Balance—precision (Extend ED224S)	Sartorius (Göttingen, Germany)
Bead mill (TissueLyser LT)	Qiagen (Venlo, Netherlands)
Biosafety cabinet (BioWizard Xtra Line)	Kojair Tech Oy (Mänttä-Vilppula, Finland)
Centrifuge (Allegra® X-30R)	Beckman Coulter (Brea, USA)
Counting chamber (Neubauer Improved, BR717805-1EA)	BRAND (Wertheim, Germany)
Fluid aspiration system (BVC control, 20727200)	VACUUBRAND (Wertheim, Germany)
Incubator (Forma™ Scientific 3250)	Thermo Fisher Scientific (Waltham, USA)
Magnetic stirrer, heated (MR Hei-Standard)	Heidolph Instruments (Schwabach, Germany)
Micro centrifuge (SD)	Carl Roth (Karlsruhe, Germany)
Microscope (DM IL LED)	Leica Camera (Wetzlar, Germany)
Multilabel plate reader (Victor™ X4)	Perkin Elmer (Waltham, USA)
Pipetters (Research™ Plus; Reference™ series)	Eppendorf (Hamburg, Germany)
Repetitive pipetter (Multipette® Plus)	Eppendorf (Hamburg, Germany)
Semi-dry blotter (PerfectBlue™ Sedec™ M)	Peqlab Biotechnologie (Erlangen, Germany)
Spacer plates (1653312)	Bio-Rad Laboratories (Hercules, USA)
Tilting shaker (WS42)	A. Hartenstein (Würzburg, Germany)
Thermo mixer (F1.5)	Eppendorf (Hamburg, Germany)
Tube roller (-)	Built in house (University medical center, Göttingen, Germany)
Tube rotator (Multi Bio RS-24)	Peqlab Biotechnologie (Erlangen, Germany)
Vortex mixer (MX-S)	DLAB Scientific (Corston, UK)

Device	Supplier
Water bath (Isotemp® 2332)	Thermo Fisher Scientific (Waltham, USA)

Table S2: Stocked laboratory consumables

Item	Supplier
6-well plate (833920)	Sarstedt (Nümbrecht, Germany)
96-well plate—black, clear bottom (3603)	Corning (New York, USA)
96-well plate—completely clear (833924)	Sarstedt (Nümbrecht, Germany)
APS (A0834)	AppliChem (Darmstadt, Germany)
Bisacrylamid 40 % (T802.1); Ethanol (9065)	Carl Roth (Karlsruhe, Germany)
BSA (04-100-810)	Paesel & Lorei (Rheinberg, Germany)
Cell Scraper (99010)	TPP (Trasadingen, Swizerland)
Chromatography Paper (3030917)	Whatman (Maidstone, UK)
DMEM (D6546)	Sigma-Aldrich (Merck, Darmstadt, Germany)
EDTA (E4884)	Sigma-Aldrich (Merck, Darmstadt, Germany)
EGTA (Titriplex® VI, 108435); NaOH (1.09913)	Merck (Darmstadt, Germany)
Glycin (A1067)	AppliChem (Darmstadt, Germany)
H2O (sterile, 06874361)	B. Braun (Melsungen, Germany)
Hanks' Balanced Salt solution (H6648)	Sigma-Aldrich (Merck, Darmstadt, Germany)
Insuline syringe (324824)	Becton Dickinson (Franklin Lakes, USA)
Laboratory film (Parafilm® M, CNP8.1)	Carl Roth (Karlsruhe, Germany)
L-glutamine (BE17-605E)	Lonza Bioscience (Basel, Swizerland)
McCoy's 5A (modified) medium (16600082); FBS (10270106)	Thermo Fisher Scientific (Waltham, USA)
Nonidet® P40 (substitute) (A1694)	AppliChem (Darmstadt, Germany)
Pasteur pipettes (747715, 747720)	BRAND (Wertheim, Germany)

Item	Supplier
Pipette tips—standard (S1110-3700, S1111-6701, S1113-170)	Starlab International (Hamburg, Germany)
Pipette tips for multipipette (0030089677)	Eppendorf (Hamburg, Germany)
Pipette tips with filter—for handling RNA (S1180-3810, S1180-4810, S1122-1830)	Starlab International (Hamburg, Germany)
Phosphatase inhibitor (PhosSTOP™, 4906837001)	Roche (Basel, Swizerland)
Protease inhibitor (Complete™, 4693159001)	Roche (Basel, Swizerland)
Proteinmarker prestained (1123YL500)	neoFroxx (Einhausen, Germany)
PVDF membrane 0.45 µm (10600023)	Cytiva (Marlborough, UK)
RNaseZAP™ (R2020)	Sigma-Aldrich (Merck, Darmstadt, Germany)
Serological pipees (86.1252.001, 86.1253.001, 86.1254.001, 86.1685.001, 86.1256.001)	Sarstedt (N¨umbrecht, Germany)
Sodium pyrophosphate (P8010)	Sigma-Aldrich (Merck, Darmstadt, Germany)
Stripping butter (ROTI®Free 2.2 plus, 3337.2)	Carl Roth (Karlsruhe, Germany)
Surface disinfectant (Optisal® N, 00-214-050)	Dr. Schumacher (Malsfeld-Beiseförth, Germany)
T-175 cell culture flask (833912002)	Sarstedt (Nümbrecht, Germany)
T-25 cell culture flasks (CC7682-4325, CC7682-4825)	Starlab International (Hamburg, Germany)
T-75 cell culture flasks (CC7682-4175, CC7682-4875)	Starlab International (Hamburg, Germany)
TEMED (A1148)	AppliChem (Darmstadt, Germany)
Tris (A1086)	AppliChem (Darmstadt, Germany)

Tubes—clear (72.704.200, 72.706.200, 72.695.200)	Sarstedt (Nümbrecht, Germany)

Item	**Supplier**
Tubes—clear (E1420-2000, E1450-1100)	Starlab International (Hamburg, Germany)
Tubes—capped (62.554.502, 62.547.254)	Sarstedt (Nümbrecht, Germany)
Tube—for ow cytometry (55.1579.002)	Sarstedt (Nümbrecht, Germany)
Tween® 20 (A4974)	AppliChem (Darmstadt, Germany)
β-mercaptoethanol (M6250)	Merck (Darmstadt, Germany)

7 References

Akimoto N, Ugai T, Zhong R, Hamada T, Fujiyoshi K, Giannakis M, Wu K, Cao Y, Ng K, Ogino S (2021): Rising incidence of early-onset colorectal cancer - a call to action. Nat Rev Clin Oncol 18, 230-243

Ashburner M, Ball CA, Blake JA, Botstein D, Butler H, Cherry JM, Davis AP, Dolinski K, Dwight SS, Eppig JT, et al. (2000): Gene ontology: tool for the unification of biology. The Gene Ontology Consortium. Nature Genetics 25, 25-29

Atsumi T, Chesney J, Metz C, Leng L, Donnelly S, Makita Z, Mitchell R, Bucala R (2002): High expression of inducible 6-phosphofructo-2-kinase/fructose-2,6-bisphosphatase (iPFK-2; PFKFB3) in human cancers. Cancer Research 62, 5881-5887

Baluk P, Hashizume H, McDonald DM (2005): Cellular abnormalities of blood vessels as targets in cancer. Curr Opin Genet Dev 15, 102-111

Barnhill R, Vermeulen P, Daelemans S, van Dam P-J, Roman-Roman S, Servois V, Hurbain I, Gardrat S, Raposa G, Nicolas A, et al. (2018): Replacement and desmoplastic histopathological growth patterns: A pilot study of prediction of outcome in patients with uveal melanoma liver metastases. J Pathol Clin Res 4, 227-240

Bentolila LA, Prakash R, Mihic-Probst D, Wadehra M, Kleinman HK, Carmichael TS, Peault B, Barnhill RL, Lugassy C (2016): Imaging of Angiotropism/Vascular Co-Option in a Murine Model of Brain Melanoma: Implications for Melanoma Progression along Extravascular Pathways. Sci Rep 6, 23834

Bertout JA, Patel SA, Simon MC (2008): The impact of O2 availability on human cancer. Nature Reviews. Cancer 8, 967-975

Boehm-Viswanathan T (2000): Is angiogenesis inhibition the Holy Grail of cancer therapy? Current Opinion In Oncology 12, 89-94

Boland CR, Goel A (2010): Microsatellite instability in colorectal cancer. Gastroenterology 138

Bray F, Ferlay J, Soerjomataram I, Siegel RL, Torre LA, Jemal A (2018): Global cancer statistics 2018: GLOBOCAN estimates of incidence and mortality worldwide for 36 cancers in 185 countries. CA Cancer J Clin 68, 394-424

Bridgeman VL, Vermeulen PB, Foo S, Bilecz A, Daley F, Kostaras E, Nathan MR, Wan E, Frentzas S, Schweiger T, et al. (2017): Vessel co-option is common in human lung metastases and mediates resistance to anti-angiogenic therapy in preclinical lung metastasis models. J Pathol 241, 362-374

Brouquet A, Abdalla EK, Kopetz S, Garrett CR, Overman MJ, Eng C, Andreou A, Loyer EM, Madoff DC, Curley SA, et al. (2011): High survival rate after two-stage resection of advanced colorectal liver metastases: response-based selection and complete resection define outcome. Journal of Clinical Oncology : Official Journal of the American Society of Clinical Oncology 29, 1083-1090

Bryant CLC, Lunniss PJ, Knowles CH, Thaha MA, Chan CLH (2012): Anterior resection syndrome. The Lancet. Oncology 13, e403-e408

Bussolino F, Mantovani A, Persico G (1997): Molecular mechanisms of blood vessel formation. Trends Biochem Sci 22, 251-256

Cantelmo AR, Pircher A, Kalucka J, Carmeliet P (2017): Vessel pruning or healing: endothelial metabolism as a novel target? Expert Opinion On Therapeutic Targets 21, 239-247

Cantelmo AR, Conradi LC, Brajic A, Goveia J, Kalucka J, Pircher A, Chaturvedi P, Hol J, Thienpont B, Teuwen LA, et al. (2016): Inhibition of the Glycolytic Activator PFKFB3 in Endothelium Induces Tumor Vessel Normalization, Impairs Metastasis, and Improves Chemotherapy. Cancer Cell 30, 968-985

Caporali A, Meloni M, Nailor A, Mitic T, Shantikumar S, Riu F, Sala-Newby GB, Rose L, Besnier M, Katare R, et al. (2015): p75(NTR)-dependent activation of NF-kappaB regulates microRNA-503 transcription and pericyte-endothelial crosstalk in diabetes after limb ischaemia. Nat Commun 6, 8024

Carmeliet P (2005): VEGF as a key mediator of angiogenesis in cancer. Oncology 69 Suppl 3, 4-10

Carmeliet P, Jain RK (2011): Principles and mechanisms of vessel normalization for cancer and other angiogenic diseases. Nat Rev Drug Discov 10, 417-427

Chang YS, di Tomaso E, McDonald DM, Jones R, Jain RK, Munn LL (2000): Mosaic blood vessels in tumors: frequency of cancer cells in contact with flowing blood. Proceedings of the National Academy of Sciences of the United States of America 97, 14608-14613

Chen H-C (2005): Boyden chamber assay. Methods In Molecular Biology (Clifton, N.J.) 294, 15-22

Clem B, Telang S, Clem A, Yalcin A, Meier J, Simmons A, Rasku MA, Arumugam S, Dean WL, Eaton J, et al. (2008): Small-molecule inhibition of 6-phosphofructo-2-kinase activity suppresses glycolytic flux and tumor growth. Molecular cancer therapeutics 7, 110-120

Clevers H (2016): Modeling Development and Disease with Organoids. Cell 165, 1586-1597

Conradi LC, Brajic A, Cantelmo AR, Bouche A, Kalucka J, Pircher A, Bruning U, Teuwen LA, Vinckier S, Ghesquiere B, et al. (2017): Tumor vessel disintegration by maximum tolerable PFKFB3 blockade. Angiogenesis 20, 599-613

Costa P, Cardoso JM, Louro H, Dias J, Costa L, Rodrigues R, Espiridiao P, Maciel J, Ferraz L (2018): Impact on sexual function of surgical treatment in rectal cancer. Int Braz J Urol 44, 141-149

Croese AD, Lonie JM, Trollope AF, Vangaveti VN, Ho YH (2018): A meta-analysis of the prevalence of Low Anterior Resection Syndrome and systematic review of risk factors. Int J Surg 56, 234-241

Cuadrado M, Martinez-Pastor B, Fernandez-Capetillo O (2006): "ATR activation in response to ionizing radiation: still ATM territory". Cell Div 1, 7

Cully M (2017): Cancer: Tumour vessel normalization takes centre stage. Nat Rev Drug Discov 16, 87

De Bock K, Georgiadou M, Schoors S, Kuchnio A, Wong BW, Cantelmo AR, Quaegebeur A, Ghesquiere B, Cauwenberghs S, Eelen G, et al. (2013): Role of PFKFB3-driven glycolysis in vessel sprouting. Cell 154, 651-663

De Oliveira T, Goldhardt T, Edelmann M, Rogge T, Rauch K, Kyuchukov ND, Menck K, Bleckmann A, Kalucka J, Khan S, et al. (2021): Effects of the Novel PFKFB3 Inhibitor KAN0438757 on Colorectal Cancer Cells and Its Systemic Toxicity Evaluation In Vivo. Cancers 13, 1011

DeClerck K, Elble RC (2010): The role of hypoxia and acidosis in promoting metastasis and resistance to chemotherapy. Front Biosci (Landmark Ed) 15, 213-225

Dekker E, Tanis PJ, Vleugels JLA, Kasi PM, Wallace MB (2019): Colorectal cancer. The Lancet 394, 1467-1480

Donnem T, Hu J, Ferguson M, Adighibe O, Snell C, Harris AL, Gatter KC, Pezzella F (2013): Vessel co-option in primary human tumors and metastases: an obstacle to effective anti-angiogenic treatment? Cancer Med 2, 427-436

Du D, Su Z, Wang D, Liu W, Wei Z (2018): Optimal Interval to Surgery After Neoadjuvant Chemoradiotherapy in Rectal Cancer: A Systematic Review and Meta-analysis. Clin Colorectal Cancer 17, 13-24

Evans SM, Koch CJ (2003): Prognostic significance of tumor oxygenation in humans. Cancer Letters 195

Fearon ER (2011): Molecular genetics of colorectal cancer. Annu Rev Pathol 6, 479-507

Finkel T, Holbrook NJ (2000): Oxidants, oxidative stress and the biology of ageing. Nature 408, 239-247

Fishel R (1998): Mismatch repair, molecular switches, and signal transduction. Genes & Development 12, 2096-2101

Fleischer JR, Schmitt AM, Haas G, Xu X, Zeisberg EM, Bohnenberger H, Küffer S, Teuwen L-A, Karras PJ, Beißbarth T, et al. (2023): Molecular differences of angiogenic versus vessel co-opting colorectal cancer liver metastases at single-cell resolution. Molecular Cancer 22, 17

Folkman J (1989): Successful treatment of an angiogenic disease. The New England Journal of Medicine 320, 1211-1212

Folkman J (2007): Angiogenesis: an organizing principle for drug discovery? Nature Reviews. Drug Discovery 6, 273-286

Franken NAP, Rodermond HM, Stap J, Haveman J, van Bree C (2006): Clonogenic assay of cells in vitro. Nat Protoc 1, 2315-2319

Fujii S, Fujimori T, Kashida H (2002): Ulcerative colitis-associated neoplasia. Pathol Int 52, 195-203

Gacche RN (2015): Compensatory angiogenesis and tumor refractoriness. Oncogenesis 4, e153

Ganesh K, Stadler ZK, Cercek A, Mendelsohn RB, Shia J, Segal NH, Diaz LA, Jr. (2019): Immunotherapy in colorectal cancer: rationale, challenges and potential. Nat Rev Gastroenterol Hepatol 16, 361-375

Gottschalk S, Anderson N, Hainz C, Eckhardt SG, Serkova NJ (2004): Imatinib (STI571)-mediated changes in glucose metabolism in human leukemia BCR-ABL-positive cells. Clinical Cancer Research : an Official Journal of the American Association For Cancer Research 10, 6661-6668

Graham JS, Cassidy J (2012): Adjuvant therapy in colon cancer. Expert Review of Anticancer Therapy 12, 99-109

Green BL, Marshall HC, Collinson F, Quirke P, Guillou P, Jayne DG, Brown JM (2013): Long-term follow-up of the Medical Research Council CLASICC trial of conventional versus laparoscopically assisted resection in colorectal cancer. Br J Surg 100, 75-82

Grinnell RS, Lane N (1958): Benign and malignant adenomatous polyps and papillary adenomas of the colon and rectum; an analysis of 1,856 tumors in 1,335 patients. Int Abstr Surg 106, 519-538

Grivennikov SI, Karin M (2010): Dangerous liaisons: STAT3 and NF-kappaB collaboration and crosstalk in cancer. Cytokine & Growth Factor Reviews 21, 11-19

Grothey A, Galanis E (2009): Targeting angiogenesis: progress with anti-VEGF treatment with large molecules. Nat Rev Clin Oncol 6, 507-518

Gupta MK, Qin R-Y (2003): Mechanism and its regulation of tumor-induced angiogenesis. World Journal of Gastroenterology 9, 1144-1155

Gustafsson NMS, Farnegardh K, Bonagas N, Ninou AH, Groth P, Wiita E, Jonsson M, Hallberg K, Lehto J, Pennisi R, et al. (2018): Targeting PFKFB3 radiosensitizes cancer cells and suppresses homologous recombination. Nat Commun 9, 3872

Hammond WA, Swaika A, Mody K (2016): Pharmacologic resistance in colorectal cancer: a review. Ther Adv Med Oncol 8, 57-84

Hanahan D, Folkman J (1996): Patterns and emerging mechanisms of the angiogenic switch during tumorigenesis. Cell 86, 353-364

Hanahan D, Weinberg RA (2011): Hallmarks of cancer: the next generation. Cell 144, 646-674

Hashizume H, Baluk P, Morikawa S, McLean JW, Thurston G, Roberge S, Jain RK, McDonald DM (2000): Openings between defective endothelial cells explain tumor vessel leakiness. The American Journal of Pathology 156, 1363-1380

Hatfield SM, Kjaergaard J, Lukashev D, Schreiber TH, Belikoff B, Abbott R, Sethumadhavan S, Philbrook P, Ko K, Cannici R, et al. (2015): Immunological mechanisms of the antitumor effects of supplemental oxygenation. Sci Transl Med 7, 277ra230

Heald RJ, Moran BJ (1998): Embryology and anatomy of the rectum. Seminars In Surgical Oncology 15, 66-71

Hendren SK, O'Connor BI, Liu M, Asano T, Cohen Z, Swallow CJ, Macrae HM, Gryfe R, McLeod RS (2005): Prevalence of male and female sexual dysfunction is high following surgery for rectal cancer. Ann Surg 242, 212-223

Hernandez Dominguez O, Yilmaz S, Steele SR (2023): Stage IV Colorectal Cancer Management and Treatment. Journal of Clinical Medicine 12

Hockel M, Schlenger K, Hockel S, Vaupel P (1999): Hypoxic cervical cancers with low apoptotic index are highly aggressive. Cancer Res 59, 4525-4528

Hu D, Pan Y, Chen G (2021): Colorectal cancer liver metastases: An update of treatment strategy and future perspectives. Surgery in Practice and Science 7

Huang Y, Goel S, Duda DG, Fukumura D, Jain RK (2013): Vascular normalization as an emerging strategy to enhance cancer immunotherapy. Cancer Research 73, 2943-2948

Huertas P (2010): DNA resection in eukaryotes: deciding how to fix the break. Nat Struct Mol Biol 17, 11-16

Hurwitz H, Fehrenbacher L, Novotny W, Cartwright T, Hainsworth J, Heim W, Berlin J, Baron A, Griffing S, Holmgren E, et al. (2004): Bevacizumab plus irinotecan, fluorouracil, and leucovorin for metastatic colorectal cancer. The New England Journal of Medicine 350, 2335-2342

Hutter-Schmid B, Humpel C (2016): Platelet-derived Growth Factor Receptor-beta is Differentially Regulated in Primary Mouse Pericytes and Brain Slices. Curr Neurovasc Res 13, 127-134

Iacopetta B (2002): Are there two sides to colorectal cancer? Int J Cancer 101, 403-408

Jabbari K, Bernardi G (2004): Cytosine methylation and CpG, TpG (CpA) and TpA frequencies. Gene 333, 143-149

Jain RK (2014): Antiangiogenesis strategies revisited: from starving tumors to alleviating hypoxia. Cancer Cell 26, 605-622

Jing X, Yang F, Shao C, Wei K, Xie M, Shen H, Shu Y (2019): Role of hypoxia in cancer therapy by regulating the tumor microenvironment. Molecular Cancer 18, 157

Kearney DE, Coffey JC (2015): A Randomized Trial of Laparoscopic versus Open Surgery for Rectal Cancer. N Engl J Med 373, 194

Keum N, Giovannucci E (2019): Global burden of colorectal cancer: emerging trends, risk factors and prevention strategies. Nature Reviews. Gastroenterology & Hepatology 16, 713-732

Keunen O, Johansson M, Oudin A, Sanzey M, Rahim SA, Fack F, Thorsen F, Taxt T, Bartos M, Jirik R, et al. (2011): Anti-VEGF treatment reduces blood supply and increases tumor cell invasion in glioblastoma. Proc Natl Acad Sci U S A 108, 3749-3754

Kim S, Chung M, Ahn J, Lee S, Jeon NL (2016): Interstitial flow regulates the angiogenic response and phenotype of endothelial cells in a 3D culture model. Lab On a Chip 16, 4189-4199

Kim W, Lee S, Seo D, Kim D, Kim K, Kim E, Kang J, Seong KM, Youn H, Youn B (2019): Cellular Stress Responses in Radiotherapy. Cells 8

Koopman M, Antonini NF, Douma J, Wals J, Honkoop AH, Erdkamp FL, de Jong RS, Rodenburg CJ, Vreugdenhil G, Loosveld OJ, et al. (2007): Sequential versus combination chemotherapy with capecitabine, irinotecan, and oxaliplatin in advanced colorectal cancer (CAIRO): a phase III randomised controlled trial. Lancet (London, England) 370, 135-142

Kuczynski EA, Vermeulen PB, Pezzella F, Kerbel RS, Reynolds AR (2019): Vessel co-option in cancer. Nature Reviews. Clinical Oncology 16, 469-493

Kuipers EJ, Grady WM, Lieberman D, Seufferlein T, Sung JJ, Boelens PG, van de Velde CJH, Watanabe T (2015): Colorectal cancer. Nat Rev Dis Primers 1, 15065

Lange MM, van de Velde CJH (2011): Urinary and sexual dysfunction after rectal cancer treatment. Nat Rev Urol 8, 51-57

Latacz E, Caspani E, Barnhill R, Lugassy C, Verhoef C, Grunhagen D, Van Laere S, Fernandez Moro C, Gerling M, Dirix M, et al. (2020): Pathological features of vessel co-option versus sprouting angiogenesis. Angiogenesis 23, 43-54

Leenders WPJ, Küsters B, Verrijp K, Maass C, Wesseling P, Heerschap A, Ruiter D, Ryan A, de Waal R (2004): Antiangiogenic therapy of cerebral melanoma metastases results in sustained tumor progression via vessel co-option. Clinical Cancer Research : an Official Journal of the American Association For Cancer Research 10, 6222-6230

Li FY, Lai MD (2009): Colorectal cancer, one entity or three. J Zhejiang Univ Sci B 10, 219-229

Liberzon A, Subramanian A, Pinchback R, Thorvaldsdóttir H, Tamayo P, Mesirov JP (2011): Molecular signatures database (MSigDB) 3.0. Bioinformatics 27, 1739-1740

Liberzon A, Birger C, Thorvaldsdóttir H, Ghandi M, Mesirov JP, Tamayo P (2015): The Molecular Signatures Database (MSigDB) hallmark gene set collection. Cell Syst 1, 417-425

Lincet H, Icard P (2015): How do glycolytic enzymes favour cancer cell proliferation by nonmetabolic functions? Oncogene 34, 3751-3759

Lopes-Coelho F, Martins F, Pereira SA, Serpa J (2021): Anti-Angiogenic Therapy: Current Challenges and Future Perspectives. International Journal of Molecular Sciences 22

Lu C-L, Qin L, Liu H-C, Candas D, Fan M, Li JJ (2015): Tumor cells switch to mitochondrial oxidative phosphorylation under radiation via mTOR-mediated hexokinase II inhibition--a Warburg-reversing effect. PloS One 10, e0121046

Lu L, Chen Y, Zhu Y (2017): The molecular basis of targeting PFKFB3 as a therapeutic strategy against cancer. Oncotarget 8, 62793-62802

Lugassy C, Kleinman HK, Vermeulen PB, Barnhill RL (2020): Angiotropism, pericytic mimicry and extravascular migratory metastasis: an embryogenesis-derived program of tumor spread. Angiogenesis 23, 27-41

Martínez-Pérez A, Carra MC, Brunetti F, de'Angelis N (2017): Short-term clinical outcomes of laparoscopic vs open rectal excision for rectal cancer: A systematic review and meta-analysis. World Journal of Gastroenterology 23, 7906-7916

Matsumoto K, Noda T, Kobayashi S, Sakano Y, Yokota Y, Iwagami Y, Yamada D, Tomimaru Y, Akita H, Gotoh K, et al. (2021): Inhibition of glycolytic activator PFKFB3 suppresses tumor growth and induces tumor vessel normalization in hepatocellular carcinoma. Cancer Lett 500, 29-40

Mazzone M, Dettori D, de Oliveira RL, Loges S, Schmidt T, Jonckx B, Tian Y-M, Lanahan AA, Pollard P, de Almodovar CR, et al. (2009): Heterozygous deficiency of PHD2 restores tumor oxygenation and inhibits metastasis via endothelial normalization. Cell 136, 839-851

Meyers BM, Cosby R, Quereshy F, Jonker D (2017): Adjuvant Chemotherapy for Stage II and III Colon Cancer Following Complete Resection: A Cancer Care Ontario Systematic Review. Clin Oncol (R Coll Radiol) 29, 459-465

Mirzayans R, Murray D (2020): Do TUNEL and Other Apoptosis Assays Detect Cell Death in Preclinical Studies? International Journal of Molecular Sciences 21

Mishra D, Banerjee D (2019): Lactate Dehydrogenases as Metabolic Links between Tumor and Stroma in the Tumor Microenvironment. Cancers 11

Moeller BJ, Richardson RA, Dewhirst MW (2007): Hypoxia and radiotherapy: opportunities for improved outcomes in cancer treatment. Cancer Metastasis Reviews 26, 241-248

Mootha VK, Lindgren CM, Eriksson KF, Subramanian A, Sihag S, Lehar J, Puigserver P, Carlsson E, Ridderstrale M, Laurila E, et al. (2003): PGC-1alpha-responsive genes involved in oxidative phosphorylation are coordinately downregulated in human diabetes. Nat Genet 34, 267-273

Muto T, Bussey HJ, Morson BC (1975): The evolution of cancer of the colon and rectum. Cancer 36, 2251-2270

Muz B, de la Puente P, Azab F, Azab AK (2015): The role of hypoxia in cancer progression, angiogenesis, metastasis, and resistance to therapy. Hypoxia (Auckl) 3, 83-92

Nouws J, Nijtmans L, Houten SM, van den Brand M, Huynen M, Venselaar H, Hoefs S, Gloerich J, Kronick J, Hutchin T, et al. (2010): Acyl-CoA dehydrogenase 9 is required for the biogenesis of oxidative phosphorylation complex I. Cell Metab 12, 283-294

Nowak-Sliwinska P, Alitalo K, Allen E, Anisimov A, Aplin AC, Auerbach R, Augustin HG, Bates DO, van Beijnum JR, Bender RHF, et al. (2018): Consensus guidelines for the use and interpretation of angiogenesis assays. Angiogenesis 21, 425-532

Park J-S, Kim I-K, Han S, Park I, Kim C, Bae J, Oh SJ, Lee S, Kim JH, Woo D-C, et al. (2016): Normalization of Tumor Vessels by Tie2 Activation and Ang2 Inhibition Enhances Drug Delivery and Produces a Favorable Tumor Microenvironment. Cancer Cell 30, 953-967

Porter AG, Jänicke RU (1999): Emerging roles of caspase-3 in apoptosis. Cell Death and Differentiation 6

Pox C, Aretz S, Bischoff SC, Graeven U, Hass M, Heussner P, Hohenberger W, Holstege A, Hubner J, Kolligs F, et al. (2013): [S3-guideline colorectal cancer version 1.0]. Z Gastroenterol 51, 753-854

Rankin EB, Giaccia AJ (2016): Hypoxic control of metastasis. Science (New York, N.Y.) 352, 175-180

Rezapour S, Bahrami T, Hashemzadeh S, Estiar MA, Nemati M, Ravanbakhsh R, Feizi MAH, Kafil HS, Pouladi N, Ghojazadeh M, et al. (2016): STC1 and NF-κB p65 (Rel A) is Constitutively Activated in Colorectal Cancer. Clin Lab 62, 463-469

Robinson JR, Newcomb PA, Hardikar S, Cohen SA, Phipps AI (2017): Stage IV colorectal cancer primary site and patterns of distant metastasis. Cancer Epidemiology 48, 92-95

Rohlenova K, Veys K, Miranda-Santos I, De Bock K, Carmeliet P (2018): Endothelial Cell Metabolism in Health and Disease. Trends In Cell Biology 28, 224-236

Ronnekleiv-Kelly SM, Kennedy GD (2011): Management of stage IV rectal cancer: palliative options. World Journal of Gastroenterology 17, 835-847

Rubenstein JL, Kim J, Ozawa T, Zhang M, Westphal M, Deen DF, Shuman MA (2000): Anti-VEGF antibody treatment of glioblastoma prolongs survival but results in increased vascular cooption. Neoplasia 2, 306-314

Rupnik A, Lowndes NF, Grenon M (2010): MRN and the race to the break. Chromosoma 119, 115-135

Salehifar E, Avan R, Janbabaei G, Mousavi SK, Faramarzi F (2019): Comparison the Incidence and Severity of Side Effects Profile Of FOLFOX and DCF Regimens in Gastric Cancer Patients. Iran J Pharm Res 18, 1032-1039

Sattler UGA, Mueller-Klieser W (2009): The anti-oxidant capacity of tumour glycolysis. International Journal of Radiation Biology 85, 963-971

Sauer R, Becker H, Hohenberger W, Rödel C, Wittekind C, Fietkau R, Martus P, Tschmelitsch J, Hager E, Hess CF, et al. (2004): Preoperative versus postoperative chemoradiotherapy for rectal cancer. The New England Journal of Medicine 351, 1731-1740

Sauer RT, Bolon DN, Burton BM, Burton RE, Flynn JM, Grant RA, Hersch GL, Joshi SA, Kenniston JA, Levchenko I, et al. (2004): Sculpting the proteome with AAA(+) proteases and disassembly machines. Cell 119, 9-18

Schneider CA, Rasband WS, Eliceiri KW (2012): NIH Image to ImageJ: 25 years of image analysis. Nature Methods 9, 671-675

Schoors S, De Bock K, Cantelmo AR, Georgiadou M, Ghesquière B, Cauwenberghs S, Kuchnio A, Wong BW, Quaegebeur A, Goveia J, et al. (2014): Partial and transient reduction of glycolysis by PFKFB3 blockade reduces pathological angiogenesis. Cell Metab 19, 37-48

Sebag-Montefiore D, Stephens RJ, Steele R, Monson J, Grieve R, Khanna S, Quirke P, Couture J, de Metz C, Myint AS, et al. (2009): Preoperative radiotherapy versus selective postoperative chemoradiotherapy in patients with rectal cancer (MRC CR07 and NCIC-CTG C016): a multicentre, randomised trial. Lancet (London, England) 373, 811-820

Seetharaman S, Etienne-Manneville S (2020): Cytoskeletal Crosstalk in Cell Migration. Trends In Cell Biology 30, 720-735

Semenza GL (2010): Defining the role of hypoxia-inducible factor 1 in cancer biology and therapeutics. Oncogene 29, 625-634

Semenza GL (2012): Hypoxia-inducible factors in physiology and medicine. Cell 148, 399-408

Serreze DV, Leiter EH, Hanson MS, Christianson SW, Shultz LD, Hesselton RM, Greiner DL (1995): Emv30null NOD-scid mice. An improved host for adoptive transfer of autoimmune diabetes and growth of human lymphohematopoietic cells. Diabetes 44, 1392-1398

Seymour MT, Maughan TS, Ledermann JA, Topham C, James R, Gwyther SJ, Smith DB, Shepherd S, Maraveyas A, Ferry DR, et al. (2007): Different strategies of sequential and combination chemotherapy for patients with poor prognosis advanced colorectal cancer (MRC FOCUS): a randomised controlled trial. Lancet (London, England) 370, 143-152

Sharma LK, Lu J, Bai Y (2009): Mitochondrial respiratory complex I: structure, function and implication in human diseases. Current Medicinal Chemistry 16, 1266-1277

Shi Y, Wang Y, Jiang H, Sun X, Xu H, Wei X, Wei Y, Xiao G, Song Z, Zhou F (2021): Mitochondrial dysfunction induces radioresistance in colorectal cancer by activating [Ca2+]m-PDP1-PDH-histone acetylation retrograde signaling. Cell Death & Disease 12, 837

Shultz LD, Schweitzer PA, Christianson SW, Gott B, Schweitzer IB, Tennent B, McKenna S, Mobraaten L, Rajan TV, Greiner DL (1995): Multiple defects in innate and adaptive immunologic function in NOD/LtSz-scid mice. Journal of Immunology (Baltimore, Md. : 1950) 154, 180-191

Siegel RL, Wagle NS, Cercek A, Smith RA, Jemal A (2023): Colorectal cancer statistics, 2023. CA: a Cancer Journal For Clinicians 73, 233-254

Siegel RL, Miller KD, Goding Sauer A, Fedewa SA, Butterly LF, Anderson JC, Cercek A, Smith RA, Jemal A (2020): Colorectal cancer statistics, 2020 US. CA Cancer J Clin 70, 145-164

Sturlan S, Oberhuber G, Beinhauer BG, Tichy B, Kappel S, Wang J, Rogy MA (2001): Interleukin-10-deficient mice and inflammatory bowel disease associated cancer development. Carcinogenesis 22, 665-671

Subramanian A, Tamayo P, Mootha VK, Mukherjee S, Ebert BL, Gillette MA, Paulovich A, Pomeroy SL, Golub TR, Lander ES, et al. (2005): Gene set enrichment analysis: a knowledge-based approach for interpreting genome-wide expression profiles. Proc Natl Acad Sci U S A 102, 15545-15550

Sung H, Ferlay J, Siegel RL, Laversanne M, Soerjomataram I, Jemal A, Bray F (2021): Global Cancer Statistics 2020: GLOBOCAN Estimates of Incidence and Mortality Worldwide for 36 Cancers in 185 Countries. CA: a Cancer Journal For Clinicians 71, 209-249

Tamas K, Walenkamp AM, de Vries EG, van Vugt MA, Beets-Tan RG, van Etten B, de Groot DJ, Hospers GA (2015): Rectal and colon cancer: Not just a different anatomic site. Cancer Treat Rev 41, 671-679

Tiefenbacher U, Wenz F (2001): [Preoperative radiotherapy combined with total mesorectal excision for resectable rectal cancer]. Strahlenther Onkol 177, 682-684

Trédan O, Galmarini CM, Patel K, Tannock IF (2007): Drug resistance and the solid tumor microenvironment. Journal of the National Cancer Institute 99, 1441-1454

van Dam P-J, van der Stok EP, Teuwen L-A, Van den Eynden GG, Illemann M, Frentzas S, Majeed AW, Eefsen RL, Coebergh van den Braak RRJ, Lazaris A, et al. (2017): International consensus guidelines for scoring the histopathological growth patterns of liver metastasis. British Journal of Cancer 117, 1427-1441

van Gijn W, Marijnen CAM, Nagtegaal ID, Kranenbarg EM-K, Putter H, Wiggers T, Rutten HJT, Påhlman L, Glimelius B, van de Velde CJH (2011): Preoperative radiotherapy combined with total mesorectal excision for resectable rectal cancer: 12-year follow-up of the multicentre, randomised controlled TME trial. The Lancet. Oncology 12, 575-582

Vaupel P, Mayer A (2007): Hypoxia in cancer: significance and impact on clinical outcome. Cancer Metastasis Reviews 26, 225-239

Vestweber D (2008): VE-cadherin: the major endothelial adhesion molecule controlling cellular junctions and blood vessel formation. Arteriosclerosis, Thrombosis, and Vascular Biology 28, 223-232

Vogelstein B, Fearon ER, Hamilton SR, Kern SE, Preisinger AC, Leppert M, Nakamura Y, White R, Smits AM, Bos JL (1988): Genetic alterations during colorectal-tumor development. The New England Journal of Medicine 319, 525-532

Vuik FE, Nieuwenburg SA, Bardou M, Lansdorp-Vogelaar I, Dinis-Ribeiro M, Bento MJ, Zadnik V, Pellise M, Esteban L, Kaminski MF, et al. (2019): Increasing incidence of colorectal cancer in young adults in Europe over the last 25 years. Gut 68, 1820-1826

Wang J-S, Wang H-J, Qian H-L (2018): Biological effects of radiation on cancer cells. Mil Med Res 5, 20

Wang Q, Shen X, Chen G, Du J (2022): Drug Resistance in Colorectal Cancer: From Mechanism to Clinic. Cancers 14

Warburg O (1956): On the origin of cancer cells. Science (New York, N.Y.) 123, 309-314

Wilson WR, Hay MP (2011): Targeting hypoxia in cancer therapy. Nature Reviews Cancer 11, 393-410

Xiao Y, Jin L, Deng C, Guan Y, Kalogera E, Ray U, Thirusangu P, Staub J, Sarkar Bhattacharya S, Xu H, et al. (2021): Inhibition of PFKFB3 induces cell death and

synergistically enhances chemosensitivity in endometrial cancer. Oncogene 40, 1409-1424

Xie Y-H, Chen Y-X, Fang J-Y (2020): Comprehensive review of targeted therapy for colorectal cancer. Signal Transduct Target Ther 5, 22

Yalcin A, Clem BF, Imbert-Fernandez Y, Ozcan SC, Peker S, O'Neal J, Klarer AC, Clem AL, Telang S, Chesney J (2014): 6-Phosphofructo-2-kinase (PFKFB3) promotes cell cycle progression and suppresses apoptosis via Cdk1-mediated phosphorylation of p27. Cell Death & Disease 5, e1337

Yancopoulos GD, Davis S, Gale NW, Rudge JS, Wiegand SJ, Holash J (2000): Vascular-specific growth factors and blood vessel formation. Nature 407, 242-248

Yang T, Xiao H, Liu X, Wang Z, Zhang Q, Wei N, Guo X (2021): Vascular Normalization: A New Window Opened for Cancer Therapies. Frontiers In Oncology 11, 719836

Yu H, Kortylewski M, Pardoll D (2007): Crosstalk between cancer and immune cells: role of STAT3 in the tumour microenvironment. Nat Rev Immunol 7, 41-51

Zheng J (2012): Energy metabolism of cancer: Glycolysis versus oxidative phosphorylation (Review). Oncology Letters 4, 1151-1157

Zhong X, He X, Wang Y, Hu Z, Huang H, Zhao S, Wei P, Li D (2022): Warburg effect in colorectal cancer: the emerging roles in tumor microenvironment and therapeutic implications. Journal of Hematology & Oncology 15, 160

Acknowledgments

I am appreciated to have a chance to pursue my doctoral degree in the field of medicine. First, I want to extend my sincerest thanks to Lena, my supervisor. She has been an exceptional mentor who has gone above and beyond in supporting me throughout my studies. She not only helped me secure my position in Germany but also provided me with accommodation and transportation upon my arrival. Her kindness, generosity, and selflessness during that challenging time made a tremendous impact on me, and I will forever be grateful for her support.

In addition to her practical help, Lena consistently encouraged me to push beyond my limits, to speak my mind, and to take bold steps in my research. Her unwavering faith in my abilities boosted my confidence and helped me become a better version of myself. Whenever I faced any obstacles or difficulties, Lena was always there to offer guidance and support, even when the reagents required for my experiments were expensive. I also appreciate Lena's willingness to accept me as a student during the COVID-19 pandemic when the world was plagued with fear and uncertainty. Despite the prevailing sentiment of xenophobia, Lena graciously welcomed me and encouraged me to integrate into the local German culture by inviting me to taste the local specialties. Her kindness and hospitality have made me feel at home and enabled me to focus on my research without any distractions.

Then, I want to take this perfect occasion to extend my profound thanks to Tiago, my post-doctoral advisor, for the exceptional support, mentorship, and genuine friendship he has provided me. Tiago has been a vital part of my academic and personal life since I arrived in Germany. He welcomed me with open arms and made me feel like a part of his family. His kindness, warmth, and care made the transition to a new country much more manageable, and I am forever grateful for his support during that difficult period.

As a teacher, Tiago was exceptional. He was patient, kind, and always willing to help in the laboratory. He was not only my teacher, but also my friend, and he always had time for me when I needed advice or guidance. Whenever I made a mistake, he never scolded me but instead taught me what I needed to do to correct it, so that I could improve and learn from my mistakes. Tiago was also my biggest supporter, and he believed in me even when I had doubts about myself. He encouraged me to aim high, to believe in my abilities, and to never

give up, even when faced with difficult challenges. His unwavering faith in me gave me the strength and confidence I needed to overcome any obstacles that came my way.

In addition to his academic mentorship, Tiago was also an excellent friend and partner. He went out of his way to ensure that I felt welcome and included in the new environment by inviting me to private parties, introducing me to his friends, and taking me to taste the local specialties. He was always there to lend a helping hand when I needed it, and I could always count on him to have my back. In conclusion, I am incredibly lucky to have met such an amazing teacher, friend, and partner like Tiago.

I want to thank to Birgit, our lab technician. Despite the language barrier, she never failed to make me feel welcome with her infectious smile and delicious baked treats. Birgit's assistance in the lab has been invaluable, and I am truly grateful for her help.

I also want to gratitude to everyone who has supported me throughout my research journey. Firstly, I want to thank my labmates, Rorbert, Teona, Olaf, Alexandra, Nick, Kaida, Fabio, Anneke, Moritz, and Dolma. Without their help, encouragement, and camaraderie, my experience in the lab would not have been as enriching and enjoyable.

Robert, my first German classmate in the lab, I am grateful for his boundless energy and patience in helping me with my lab problems and correcting my English pronunciation. Teona, my labmate from Georgia, thank you for your company, encouragement, and support during both the happy and anxious times we spent together in the lab. Olaf, your clear and complete experimental results have always been impressive, and your willingness to remotely coach me on data analysis after finishing your lab semester is much appreciated. Alexandra, your inner strength and constant smile in the face of work and study pressure are truly admirable. Nick, thank you for being a sophisticated and serious inspiration to me, keeping me motivated in the face of failures and unsatisfactory experimental results. Kaida, your sweet and kind-hearted nature, combined with your dedication to hard work and study, is truly inspiring. Fabio, your soft-hearted and knowledgeable nature has taught me many useful skills, and I am grateful for your patience in answering my questions. Anneke, your hard work, and dedication to the lab have been crucial in completing my fluorescent stained section photos and analysis results. Moritz, your insistence on not missing lunch and your conscientious and responsible approach to work are much appreciated, as is your gentle and caring nature toward your classmates. And Dolma, my good friend who provided me with patience, help, and encouragement.

I also want to thank Gwen, and all my other close classmates who have been a great help to me throughout my research journey. Their support and guidance have been invaluable. Theon and Kaiven for both of your invaluable assistance in formatting and revising my paper.

I want to thanks to my parents, sister. And to my dear friends, Nada, Roberto, Xuhongmiao, and Luowanhui, thanks for your support and encouragement.

To all those who have touched my life during this journey, I offer my deepest gratitude. Thank you for the memories, the knowledge, and the experiences that have made these past years so unforgettable.